NEUROTROPISM OF THEILER'S MURINE ENCEPHALOMYELITIS VIRUS

A Thesis

by

DORISSA VILLARREAL

Submitted to the Office of Graduate Studies of
Texas A&M University
in partial fulfillment of the requirements for the degree of

MASTER OF SCIENCE

August 2005

Major Subject: Veterinary Microbiology

NEUROTROPISM OF THEILER'S MURINE ENCEPHALOMYELITIS VIRUS

A Thesis

by

DORISSA VILLARREAL

Submitted to the Office of Graduate Studies of
Texas A&M University
in partial fulfillment of the requirements for the degree of

MASTER OF SCIENCE

Approved by:

Chair of Committee,	Jane Welsh
Committee Members,	Ralph Storts
	Luc Berghman
Head of Department,	Anne Kier

August 2005

Major Subject: Veterinary Microbiology

ABSTRACT

Neurotropism of Theiler's Murine Encephalomyelitis Virus. (August 2005)

Dorissa Villarreal, B.S., Texas A&M University

Chair of Advisory Committee: Dr. Jane Welsh

Theiler's murine encephalomyelitis virus (TMEV) can infect the central nervous system (CNS) and cause neurological damage. The exact route by which TMEV enters the CNS remains unknown. Two hypotheses suggest that TMEV enters the CNS either by the neural and/or the hematogenous pathway. To explore these hypotheses, the GDVII strain of Theiler's virus was inoculated via different routes in susceptible mice. The incidence of paralysis and/or encephalitis was evaluated. The forms of paralysis displayed corresponded to the site of viral inoculation. Following intramuscular (i.m.), intraperitoneal (i.p.), intravenous (i.v.) and footpad routes of injection, bilateral and or contralateral paralyses were observed. In mice injected intratongue, tongue paralysis was observed. Intracranial (i.c.) injections resulted in 100% mortality. A detailed time course experiment was also completed which focused on the neural transport pathway used by TMEV to invade the CNS. The GDVII strain of Theiler's virus was injected into the left gastrocnemius muscle and the hypoglossal nerve (CN XII). The incidence of paralysis and/or encephalitis was evaluated on the basis of clinical signs, immunofluorescent analysis, and histopathology. Following the i.m., route of injection, unilateral hind limb paralysis was observed in the injected limb and a weakening of the

contralateral limb was also observed. In mice injected in the hypoglossal nerve, tongue paralysis was observed. Also, the penis of most affected males was prolapsed. The localization of viral antigen using fluorescent labeling correlated with the clinical signs of paralysis for both injections. The studies reported here support the theory that GDVII Theiler's virus may gain access to the CNS through a neural transport pathway.

ACKNOWLEDGEMENTS

I would like to thank my committee chair, Dr. Jane Welsh, and my committee members, Dr. Ralph Storts, and Dr. Luc Berghman. I would also like to thank Dr. Colin Young. They provided me with their guidance and assistance in my research. I would like to thank Dr. Larry Johnson for giving me the opportunity to be a part of the PEER NSF Fellowship.

I would also like to give special thanks to Dr. Robert Burghardt and Dana Dean for their assistance and instructions with my research. I would like to thank Wentao Mi, Andrew Steelman, and other members in my lab for their support and friendship. Lastly, I would like to thank my family and friends for their love.

TABLE OF CONTENTS

Page

LIST OF FIGURES

FIGURE Page

LIST OF TABLES

INTRODUCTION

History

Motor neuron disease is a term applied to neurodegenerative diseases that involve a loss of lower motor neurons and/or upper motor neurons of the central nervous system (CNS) [1]. The clinical signs associated with motor neuron diseases are characterized by a progressive weakening of the skeletal muscle affected that leads to atrophy and paralysis. Many studies suggest that the onset of motor neuron diseases can be associated with a number of factors. These include infectious etiology, genetic inheritance, and environmental triggers [2]. At the present time there is no cure for these types of neurological diseases, however, the use of animal models of motor neuron diseases have provided an understanding of their causes and the pathogenesis.

One notable model of importance is Theiler's Murine Encephalomyelitis Virus (TMEV) infection in mice. Max Theiler, a South African – American research physician, originally isolated TMEV in 1933 from the CNS in mice that developed flaccid paralysis of the hind limbs [3]. Following this observation, he reproduced these results by injecting mice via intracranial and intranasal sites [3,4]. The mice developed paralysis within weeks post infection, and he also observed lesions in the ventral horn of the spinal cord. He used his discovery as an animal model of human poliomyelitis. Theiler is largely known for his work on TMEV and yellow fever.

This thesis follows the style of Microbial Pathogenesis.

In 1951, he was awarded the Nobel Prize in Medicine for his work on yellow fever. Following his pioneering work on TMEV, new strains have been isolated that have the capability of persisting in the CNS and causing an inflammatory disease of the CNS [5]. The inflammatory demyelination of the CNS seen in TMEV resembles Multiple Sclerosis, and is used as an animal model for this disease. The significance of this model system for studying Multiple Sclerosis and other neurological diseases is that the model is well characterized and the virus will readily infect susceptible mice. Also, because it only affects genetically susceptible mice it can be used as an animal model of neurological diseases caused by genetic factors. Lastly, it is an excellent model to study immune-mediated pathogenesis.

Virology of Theiler's virus

Theiler's murine encephalomyelitis virus TMEV is a member of the *Picornaviridae* family and belongs to the genus cardiovirus [6]. The genome of Theiler's virus is an 8 kb-long positive strand RNA molecule. After entry of the virus into the host cell, it will immediately begin the replication cycle in the host cell cytoplasm. The RNA strand is polyadenylated at the 3' end. At the 5' end it contains a small protein covalently linked termed, VPG [7]. TMEV RNA includes a large open reading frame that encodes a 2000 amino acid – long polyprotein. During translation, the chain is cleaved into 12 mature proteins by autoproteolytic activity. Translation of the open reading frame is initiated by the internal ribosome entry site located at the 5' non-coding region. The persistent strains of TMEV have an additional open reading frame that encodes an 18-kDa leader (L) protein. The function of the L protein was

shown to facilitate in the infection of Theiler's virus and viral persistence [8, 9]. TMEV also contains 4 polypeptide chains VP1, VP2, VP3, and VP4 that assemble to form the viral capsid (Fig. 1). The role of protein 2A is unknown; however, some picornaviruses such as poliovirus use 2A to cleave VP1 from the newly translated polyprotein [7]. 3B also termed VPG is covalently linked to the 5' end, and 3B is used during encapsulation and replication. 3C is the proteinase that is responsible for the majority of the polyprotein cleavages. 3D is the RNA-dependent RNA polymerase, and proteins 2B, 2C, and 3A are used in the replication cycle (Fig. 1).

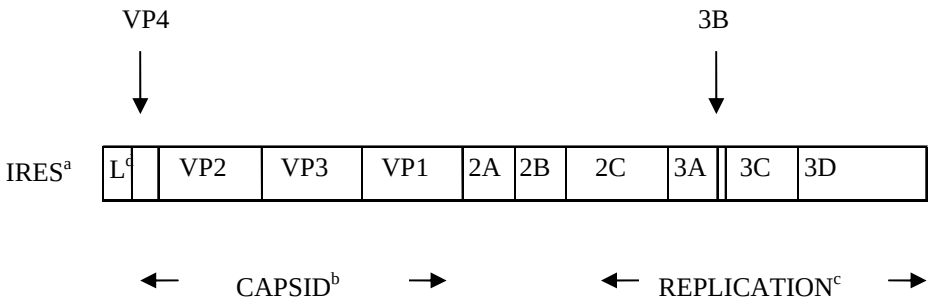

Figure 1. Theiler's virus genomic organization.
[a] IRES at 5' end for translation initiation
[b] polypeptide chain, VP1, VP2, VP3, & VP4, used in capsid assembly
[c] proteins 2A, 2B, 2C, 3A, 3B, 3C, & 3D used in replication cycle
[d] L protein function largely unknown

Classification of Theiler's virus

Theiler's virus is a naturally occurring enteric pathogen of mice and in early disease causes poliomyelitis-like flaccid paralysis in mice [6]. Theiler's viruses are divided into two subgroups: GDVII and Theiler's Original (TO). The GDVII group is extremely neurovirulent and induces acute fatal polioencephalomyelitis without demyelination. The TO group is less neurovirulent and includes the BeAn and DA strains. These strains cause a biphasic disease in which the early phase is characterized by an acute encephalomyelitis. If the virus persists, the animals will develop a chronic demyelinating disease in the CNS. This phase resembles multiple sclerosis in humans, and therefore is used as an animal model [5].

The mechanism behind the ability of GDVII virus to primarily infect neurons in the gray matter, but not infect glial cells in the white matter of the spinal cord is largely unknown. In contrast, the DA virus has the ability to infect neurons in the gray matter during the acute phase and persistently infect glial cells and macrophages in the white matter during the chronic phase. Although this suggests GDVII may not have the ability to travel along axons effectively, GDVII strain has been shown to be transported along axons by other experiments [10, 11, 12]. Attenuated GDVII strains that were obtained by mutations on the 5' noncoding region of the genome do not kill the host, however, they are unable to persist in the host [13]. One study suggests that differences between DA and GDVII are possibly due to the severity and rapid degeneration of axons does not allow the transport and spread of GDVII from the gray matter to the white matter. In this study immunohistochemical analysis of axonal pathology indicates axonal injury in

both DA and GDVII; however the extent of injury in the acute phase of DA compared to GDVII infection, indicates slower development of axonal injury [12]. Other studies demonstrate difference(s) in the virus-host receptor-binding site between GDVII and DA viruses that may contribute to the difference in host cell tropism and species specificity. Several studies have mapped the regions of the viral genome responsible for persistence and demyelination at the surfaces of the capsid [14, 15]. Some studies show that persistent but not neurovirulent strains of Theiler's virus use sialic acid for entry [14].

Pathogenesis

Theiler's Murine Encephalomyelitis virus (TMEV) is a natural enteric pathogen of mice that causes asymptomatic infection. In rare occasions the virus will invade the central nervous system (CNS) and cause neurological disease. The mechanism of entry of TMEV to the CNS is unknown. However, studies with poliovirus, the causative agent of poliomyelitis in humans, and like TMEV is within the Picornaviridae family [16], has shown that TMEV shares many biological characteristics in common with poliovirus. Similar to TMEV, in nature, poliovirus is spread from host to host via the fecal-oral route or the oropharyngeal-oral route [17, 18]. After ingestion the virus replicates in the walls of the pharynx or the lower gastrointestinal tract, spreads to local and regional lymphatic tissue, and then invades the blood stream before penetrating and replicating in the nervous system [19]. However, it may be possible after alimentary infection, for poliovirus to infect the regional ganglia cells and then invade the nervous system.

Two hypotheses suggest that TMEV enters the CNS either by the neural and/or the hematogenous pathway. It is postulated that invasion of the CNS by TMEV is via

the circulation and crossing the blood-brain barrier (BBB) or through lymphatic channels [20]. The BBB is composed of specialized cerebrovascular endothelial cells, which restrict vesicular transport and protect the CNS from harmful substances circulating in the blood. Hematogenous virus entry into the CNS may involve endothelial cells and/or macrophages. Viral RNA of TMEV has been detected in vascular endothelial cells, neurons and glial cells in the brains and spinal cords [21]. TMEV has also been shown to replicate in brain endothelial cells in vitro [22]. Moreover, mononuclear cells isolated directly from the CNS inflammatory infiltrates of TMEV infected mice were found to contain infectious viral antigens, and TMEV was found to replicate in brain macrophages. This experimental evidence strongly suggests that TMEV may enter the CNS through the hematogenous circulation and cross the BBB by infecting and replicating in the endothelial and/or inflammatory cells.

Studies with poliovirus (PV) suggest that after i.v inoculation, poliovirus may enter the CNS through the BBB at a fairly high rate although it is not known how poliovirus permeates the BBB[17]. One experiment using human poliovirus receptor (hPVR) supports the hematogenous pathway. For instance, hPVR was expressed on monocyte/macrophages from peritoneal samples. In addition, 26–32% of hPVR transgenic bone marrow and spleen cells express CD155 poliovirus receptor (PVR) on monocyte/macrophages, T cells and hematopoietic precursor cells [23]. The identification of PV in monocytes may provide insight into PV pathogenesis, such as transport of the virus into the CNS. These findings also indicate that these cells might be involved in poliovirus replication during poliomyelitis.

Several studies also suggest that the main viral dissemination route for Theiler's virus may occur by infection of peripheral organs, such as muscle, followed by viral entry from these secondary sites via peripheral neural routes [10, 11, 12, 24]. One particular study injected virus in the left hind limb of susceptible mice. Upon, histological analysis the spread of GDVII virus from the periphery to the inferior spinal cord through the sciatic nerve and then the anterior spinal cord segment was evident. After nerve transection of the sciatic nerve no viral RNA was detected in the inferior spinal cord up to 4 days p.i [10]. These findings suggest that the mechanism of transport of the GDVII virus is by fast axonal transport. CNS infection may occur by infection of skeletal muscle followed by entry of the virus via peripheral neural routes. Myelinated motor nerves branch out from the CNS and innervate skeletal muscles. TMEV may infect the motor neurons, and then be transported retrogradely along the axons of motor neurons and hence to invade the central nervous system. The study of entry into the CNS and dissemination of the virus in the CNS is important in understanding the disease pathogenesis.

Mice injected via the intracranial route with GDVII Theiler's virus do not develop paralysis [3,4]. This is a consequence of the high neurovirulence of GDVII in susceptible mice. However, the distribution of DA virus, a less neurovirulent strain of TMEV, in the spinal cord after intracerebral inoculation has been evaluated by immunohistochemistry [25]. In the early stage of infection viral antigens were detected in the motor neurons of the anterior horn. TMEV may gain access to the anterior horn cells from the brain through the corticospinal tract or the ventral root entry zone.

Immunohistochemical analysis detected viral antigens in glial cells of the corticospinal tract, which would support the neuronal route [25]. However, entry of TMEV to the anterior horn of the spinal cord may allow access through the ventral root entry zone. The blood-brain barrier in this region is more “leaky” and may be vulnerable during viral infection [20]. In addition, within the anterior horn the axons of motor neurons are composed mainly of ventral roots. This is consistent with retrograde invasion from the ventral nerve entry zone to the anterior horn cells [25]. The presence of viral RNA in the endothelial cells of blood vessels was also identified in this study [25].

Experiments using neonatal mice to demonstrate the route of viral spread from the gastrointestinal tract to the CNS were performed [26]. Using kinetic analysis, viral titers were used to measure viral spread in mice inoculated orally with the DA strain. These results showed higher titers in well-vascularized tissues such as the spleen and liver compared to the CNS [26]. Moreover, pathological studies revealed that infected neurons were found in areas of the CNS that are not directly connected via axons to peripheral organs, such as the muscle. After intranasal inoculation with poliovirus, the virus spreads to the hypothalamus, from there to the thalamus and, hence through the spinothalamic tract, to the lumbar cord [27]. However monkeys can no longer be infected with poliovirus if the olfactory bulbs or tracts were removed, or the neuronal pathway was inhibited by chemical agents such as aluminum sulfate, nitrophenol, trinitrocresol, mercurochrome or zinc sulfate [27].

Neuropathology of TMEV

Following intracranial injection of GDVII, inflammatory infiltrates of the leptomeninges can be seen as early as 1- 2 days post infection (3, 4, 6). The inflammatory infiltrates seen consist of lymphocytes and monocytes/macrophages [6]. An acute viral encephalomyelitis is evident with an intense inflammatory mononuclear cell infiltrate in the gray matter. No lesions are seen in the white matter. Perivascular mononuclear cell infiltrates are also present. After some time the infected neurons start to undergo degenerative changes or cell death by apoptosis.

Cell death by apoptosis usually occurs in isolated cells, and does not disrupt other living cells surrounding it [28]. This process is sometimes referred to as programmed cell death because it requires initiating signals of a cell to undergo apoptosis that can come from outside or inside the cell. Also, sequential activation of proteases serves to amplify the signal and allow a rapid end to the cell. The mitochondria also play an important role in that it serves to integrate several signals for apoptosis. The morphological appearances of a normal cell undergoing apoptosis are distinct. Once the normal cell receives overriding signals to undergo apoptosis it first appears irregularly contoured and shrunken away from neighboring cells [28]. Pyknosis then occurs, which is characterized by the nuclear chromatin undergoing dense condensation. Small pieces of the cell containing condensed chromatin begin to break off into apoptotic bodies. In light microscopy apoptotic bodies have dense nuclear chromatin with little eosinophilic cytoplasm, and are clearly separated from surrounding cells. The pieces then are taken up by phagocytic cells especially macrophages, and they

are gradually ingested. The significance of macrophages in the removal of apoptotic bodies lies in the macrophages ability to ingest these bodies without the release of cellular constituents, thereby causing no inflammatory response. Macrophages are derived from blood monocytes that migrate out of the blood vessel and have become activated in the tissue in response to certain chemotaxic stimuli [29].

Cells of the immune system

Inflammation is the tissues response to irritation or injury. It allows defensive factors to gain access to the site of irritation or injury. The cells of the immune system circulate throughout the blood and lymphatic channels [29]. The cells will migrate to tissues in response to a pathogen or injury. The type of cells found in a particular tissue is important to understanding the type of injury involved. Microbial infections, hypersensitivity reactions, physical agents, chemicals, and tissue necrosis may instigate the onset of acute inflammation [29]. The essential physical characteristics of acute inflammation are redness of inflamed tissue, increase in temperature due to increase blood flow, swelling due to the accumulation of edema fluid in the extravascular space, and pain due to inflammatory edema [30]. Loss of function may also be a consequence of acute inflammation due to the pain and swelling. The cells mainly seen in the early immune response to an antigen are mast cells, dendritic cells, neutrophils, monocytes/macrophages, and natural killer cells (NK) [29]. Although there is degree of overlap between the early immune response and the later acquired immune response, immune cells, B lymphocytes and T lymphocytes, infiltrate lesions later [29]. The

clinical signs described earlier are due to systemic effects induced by these cells and tissue mediators, which will be discussed in the next few paragraphs.

Mast cells circulate in the blood, but are mainly found in the connective tissue of the skin, gastrointestinal tract and respiratory tract [29]. They are large, round cells, whose cytoplasm is packed with large granules. Upon stimulation with complement components they release inflammatory mediators stored in their granules [29]. One inflammatory mediator released is histamine. Histamine is a vasoactive factor causing dilation of arterioles and enhancing the early phase of vascular permeability of venules. Mast cell secretion of histamine causes the release of TNF-α from macrophages. The effect of these substances increases vascular permeability and therefore contributes to the acute inflammatory response [29]. Mast cells are well known for their roll in allergic responses. However, they also express several pattern recognition molecules that can alter the immune response, and can respond to both bacterial and viral products.

The neutrophils contain granules in their cytoplasm that stain pink with H&E. They are predominately phagocytic cells of the early immune system that usually are evident in high numbers with bacterial infections [29]. They destroy bacteria, and cell debris through a process called phagocytosis. In phagocytosis the neutrophil flows over and binds to foreign material. It is then drawn into the cell where the cytoplasm then encloses it in a phagosome. Lysosome of the neutrophil attaches to the phagosome, and releases enzymes into it that break down and digest the foreign material. They are mainly found circulating in the blood. The initiation of neutrophils into the extracellular space is mediated by a change in blood cell flow within the lumen of the larger blood

vessels [30]. Normally blood cells flow in the center of the lumen while plasma flows near the vessel walls, however, a loss of intravascular fluid and an increase in plasma thickness causes a slowing of blood flow. This allows neutrophils to occupy positions along endothelial surfaces. Once neutrophils are along sites of injury they come into contact with adhesion molecules [30]. There are several types of adhesion molecules that are increased by chemical inflammatory mediators. Some act as lectins that bind to carbohydrates on leukocytes. These surface adhesion molecules may be expressed by complement components, leukotriene B4, and tumor necrosis factor. Other classes are called selectins which establish the first loose contact between leukocytes and endothelium resulting in the rolling action. Also, included among adhesion molecules are integrins, and intercellular adhesion molecule–1. These increase the leukocyte-endothelium surface adhesion molecule bond. The expression of selectins is mediated by interleukin-1, endotoxins, and tumor necrosis factor.

Macrophages are derived from blood monocytes that migrate out of the blood vessel and have become activated in the tissue in response to chemotaxic stimuli as described earlier [29,30,31]. Macrophages belong to a group of the mononuclear phagocytic system. Unlike neutrophils, inflammatory macrophages are able to undergo phagocytic activity repeatedly, and can remove dead, dying and damaged tissue. Macrophages can also process and present material to lymphocytes. Additionally, macrophages secrete numerous chemical mediators. Although macrophages do have this capability, dendritic cells are specialized cells whose main function is to take up antigen

and display it for recognition by lymphocytes. They circulate in the blood and are also found in the tissues.

In nervous tissue, microglia are regarded as bone marrow derived monocytes that enter the central nervous system (CNS) in the early stages of development [32]. A number of microglia are able to actively phagocytose, process and present antigens to immune cells. MHC class II molecules have been detected in resident microglia [32]. More specifically, there is an increased expression of MHC class II molecules on microglia that have been exposed to pro-inflammatory cytokines [32]. Microglia are sources of cytokine production such as IL-10 and IL-15 that regulate the response of cells in the adaptive immune system. They express CD14 receptor for lipopolysaccharide, which is a cell wall component of gram-negative bacteria [32]. Due to their ability to process and present antigens and induce immune responses they can significantly compromise the blood-brain barrier (BBB) [32].

Natural killer cells are T cell precursors that contain cytotoxic molecules [29]. These molecules include perforin and granzyme that are capable of killing virally infected cells [29]. These cells are activated by IL-12 secreted by macrophages. Unlike T cells they do not need to recognize specific epitopes of viral antigen, and therefore are a part of the early immune response. In contrast, the later acquired immune response includes B cells and T cells. B cells differentiate into plasma cells that secrete antibodies [29]. T cells can differentiate into cytotoxic T cells, that kill virally infected cells, or they can differentiate into T cells that activate B cells and macrophages [29].

T cells infiltrating the CNS are those that have been recently activated or memory cells. Moreover, only T cells that express specificity to CNS antigens are retained within the brain parenchyma [32]. Upon activation newly expressed adhesion molecules direct T cells to inflamed sites. T cells express adhesion molecules, integrins, and intercellular adhesion molecule–1 [33], which increases the leukocytes-endothelium surface adhesion molecule bond. These are a group of selectins that are chemically mediated by interleukin-1, endotoxins, and tumor necrosis factor [33]. After, binding to the endothelial surface, inflammatory cells migrate through the walls of venules and small veins [33]. T cell infiltrates followed by other inflammatory cell infiltrates such as monocytes are another source of pro inflammatory mediators that are highly regulated in the brain and spinal cord [32].

OBJECTIVES

The exact route by which TMEV enters the CNS remains, for the most part, unknown. Two hypotheses suggest that the virus enters the CNS either by the neural and/or the hematogenous pathway. To explore these hypotheses, a preliminary study was done that focused on understanding the mechanisms of entry of Theiler's virus GDVII into the CNS using different sites of exposure, and the pathway the virus takes once in the CNS. The following inoculation sites using GDVII strain were carried out: intramuscular (i.m.), intraperitoneal (i.p.), intrafootpad, intratongue, intracranial (i.c.) injections, and intravenous (i.v.) injections. The results obtained in this preliminary experiment showed that TMEV is capable of accessing the neural route with out accessing the hematogenous route.. Additionally, once TMEV enters the CNS it is capable of traveling throughout the CNS via the nervous circuitry. The neural transport pathway hypothesis was further tested in this thesis. In particular a time course experiment was performed following injection of the hypoglossal nerve, or 12^{th} cranial nerve, and injection of the left gastrocnemius muscle.

To explain the route of entry and dissemination pathway involved in TMEV pathogenesis, the virus was injected intramuscularly into the left gastrocnemius muscle of susceptible mice. A detailed time course experiment was performed using the GDVII TMEV strain, which was injected into the left gastrocnemius muscle of 4-week-old male CBA mice. After injection, the mice were sacrificed on days one, two, three, four, five, and six post-infection. Mice injected with GDVII TMEV were also observed for any incidence of paralysis including rear and/or fore limb paralysis up until the time of

sacrifice. Histopathological evaluation was carried out on the mice following intramuscular injection with GDVII Theiler's virus. Histopathological examination of the CNS of all mice was evaluated by observing the severity of inflammation present on the different days of post infection. The CNS lesions include mononuclear cell infiltrates and perivascular cuffing. The correlation between the extent of neuronal destruction and the severity of rear limb paralysis and/or fore limb was also evaluated. The specific neurotransmission of TMEV in the spinal column to the medullary areas of the brain was determined by immunofluorescence studies using a purified polyclonal rabbit anti-GDVII virus.

To explain the route of entry and dissemination pathway, an intranerve injection of TMEV into the 12^{th} cranial nerve of susceptible mice was also performed. A detailed time course experiment using the GDVII TMEV strain was performed by injecting in the 12^{th} cranial nerve, the hypoglossal nerve. After injection, a total of four mice were sacrificed on days one, two, three, four, five, six, and seven post-infection. Mice injected with GDVII TMEV were also observed for any incidence of paralysis, including tongue paralysis. Histopathological evaluation was also carried out on the mice following hypoglossal nerve injection with GDVII Theiler's virus. Any evidence of mononuclear cell infiltrates and perivascular cuffing was noted. The correlation of the extent of neuronal destruction in the brain with the tongue paralysis and/or other clinical signs was evaluated. The specific neurotransmission of TMEV into the medullary areas of the brain and also in the spinal cord was determined by immunofluorescence studies using a purified polyclonal rabbit anti-GDVII virus.

RESULTS

Preliminary experiment gastrocnemius muscle injection of TMEV

Experimental evidence indicates a possibility of CNS invasion of TMEV by infection of skeletal muscle followed by entry of the virus via peripheral neural routes. Mice injected with GDVII Theiler's virus into the left gastrocnemius muscle showed signs of paralysis. Mice injected with GDVII Theiler's virus into the left gastrocnemius muscle showed flaccid paralysis between day 2 and 4 p.i. The initial state of paralysis was first observed in the injected rear limb. Most mice showed weakness or unilateral flaccid paralysis on the injected rear limb by day 3 p.i. A corresponding paralysis of the contralateral limb is seen in 100% of mice that are initially injected in the left gastrocnemius muscle with GDVII virus. Weakening of the contralateral rear limb was evident on day 4, and by day 5 p.i. bilateral paralysis on both rear limbs was evident. Usually one of the fore limbs showed involvement by day 6 p.i. The results indicate that the spread of GDVII virus may occur from the periphery to the inferior spinal cord. The virus then travels along interneurons where it then crosses over to the contralateral limb. If this paralysis was allowed to progress mice usually developed complete bilateral forelimb and bilateral rear limb paralysis by day 6 p.i. The incidence of paralysis for GDVII Theiler's virus was 100%, therefore all injected mice showed paralysis.

Preliminary experiment intrafootpad injection of TMEV

Results obtained from mice injected into the left footpad had similar results as those of the i.m. injections with GDVII. The GDVII virus can infect and kill CNS neurons efficiently. It is able to spread from the periphery to the spinal cord through the

sciatic nerve were it will cause paralysis initially in the inoculated limb. All mice were injected with GDVII strain in the left hind footpad and were examined daily for clinical signs. The typical course of the disease was paralysis of the inoculated limb 2 to 4 days p.i., followed by contralateral rear limb paralysis 1 to 2 days p.i. Unilateral forelimb paralysis was also evident by day 6 p.i. These results were consistent with those results obtained from i.m. injections; indicating the spread of the GDVII strain from the periphery to the CNS via the sciatic nerve.

Preliminary experiment intraperitoneal of injection of TMEV

Upon i.p. injection of GDVII Theiler's virus into the peritoneal cavity mice developed flaccid paralysis either in the rear limbs and/or the fore limbs. Most infected mice developed paralysis in the rear-limb first, and by day 6 p.i. all mice developed fore and rear limb paralysis. The percentage of mice that developed flaccid paralysis was 100%. There are a few possibilities of CNS invasion by means of the i.p route. Viral entry through the abdominal sympathetic trunk, which supplies preganglionic fibers throughout the abdominal and pelvic regions, is one possibility. Other possibilities include direct invasion of the CNS from the bloodstream, or by infection of peripheral organs, such as muscle, followed by viral entry from these secondary sites via peripheral neural routes.

Preliminary experiment intravenous injection of TMEV

Mice inoculated directly into the bloodstream with GDVII Theiler's virus showed flaccid paralysis either in the rear limbs and/or the fore limbs. Most infected mice developed weakening in the rear-limb and forelimb by day 3 p.i. Mice infected

usually fully developed paralysis by day 4 p.i. Following the intravenous injection with GDVII Theiler's virus 80% of the mice showed at least one form of paralysis.

Preliminary experiment intracranial and intratongue injection of TMEV

All mice inoculated i.c. with GDVII Theiler's virus died within 48 hrs p.i. Clinical signs of encephalitis were evident within 24 hrs. Clinically, encephalitis was observed by neck and arched back, and a ruffled fur appearance. All mice injected with GDVII Theiler's virus intratongue develop tongue paralysis by day 4 p.i. Other clinical results were similar to those for the intracranial injection. The clinical signs in mice injected in the tongue were arched back, ruffled fur, and tongue paralysis.

Preliminary experiment histopathological studies

Histopathological review was performed following most routes of injection with GDVII Theiler's virus. Following, intravenous and intraperitoneal routes of injection mice were sacrificed by day 6 p.i. Following, intramuscular, intratongue, and intrafootpad route of injection mice were sacrificed by day 6 p.i. Following, intracranial inoculation mice were found dead by day 2 p.i. or administered a lethal dose of anesthetic. Upon histological examination a varying severity of inflammation was present between different routes of injection. The lesions present in the CNS included mononuclear cell infiltrates and perivascular cuffs. The extent of neuronal destruction was consistent with the severity of rear limb paralysis and/or forelimb paralysis. The non-infected group did not show any evidence of microgliosis or perivascular cuffing (Fig. 2 (A)).

Of the animals that displayed bilateral hind limb paralysis histopathological evaluation indicated that there was inflammatory infiltration in the gray matter of the left and right anterior horn (Fig. 2 (B)). Inflammatory mononuclear infiltrates as well as degenerated and necrotic neurons in the gray matter of the left and right anterior horn in the upper lumbar segment of the spinal cord were evident (Fig. 2 (C, D)). The mice that displayed forelimb paralysis had a significant amount of inflammatory infiltrates and neuronal loss in the cervical spinal cords (Fig. 2 (F)). The mice that showed bilateral rear limb and unilateral forelimb paralysis histopathological evaluation indicated that inflammation was apparent throughout the lumbar and cervical sections of the spinal cord (Fig. 2 (E, F)). In the spinal cord meningitis was most prominent in i.m., i.f., i.v., and i.p. injections. Small patchy areas of inflammatory infiltrates were seen in most routes of injection. Inflammation did not appear to be confined to a specific area.

The severity and distribution of lesions in the spinal cord correlated with clinical disease. Paralyzed animals invariably showed inflammation and neuronal degeneration in the spinal cord of paralyzed mice. Moreover, the sites of lesions in the spinal cord of paralyzed animals consistently corresponded to the distribution of clinical paralysis.

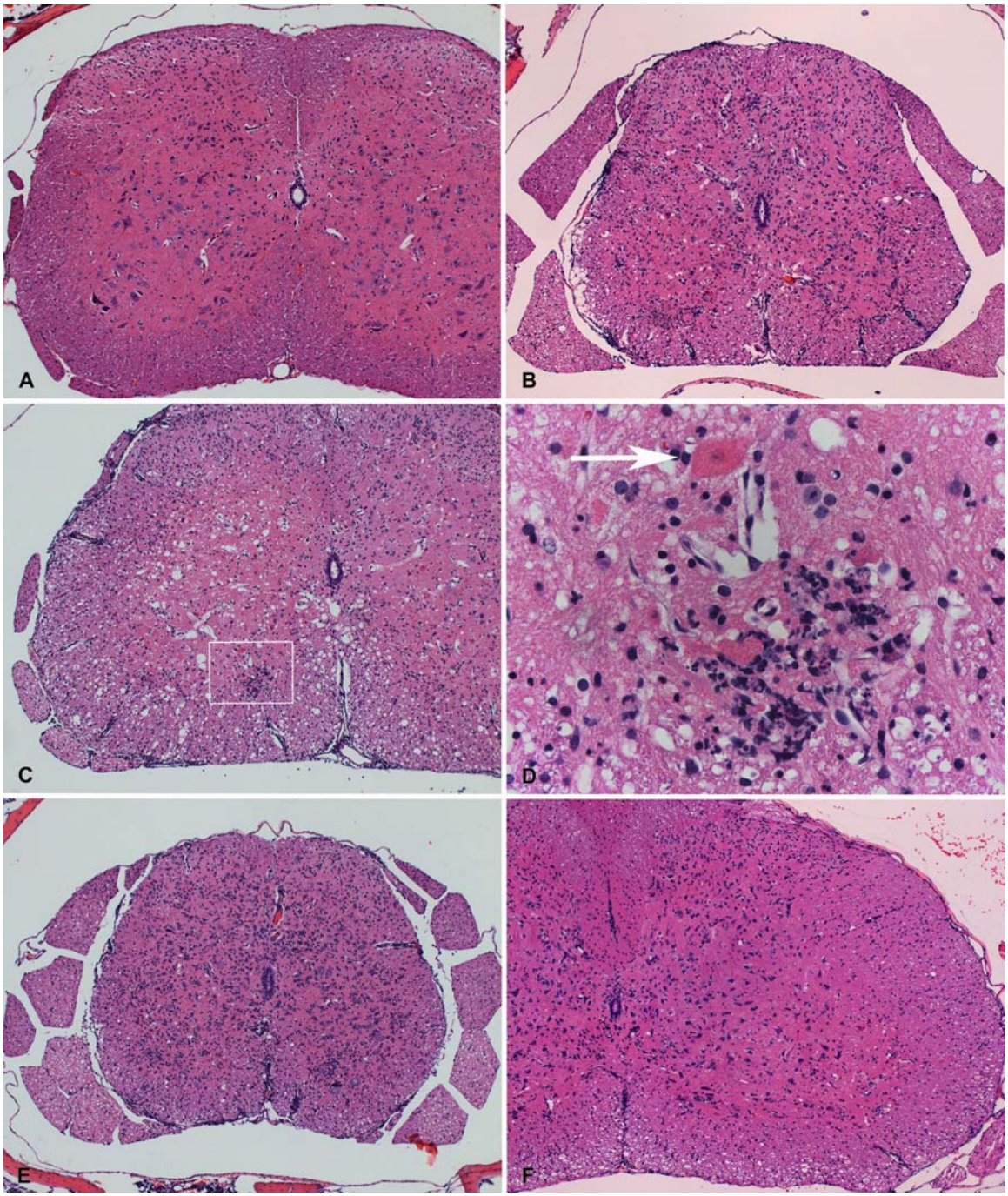

Figure 2. H&E photomicrographs of cross sections of spinal cord sections in preliminary experiment. Panels A, B, C, E, & F were taken at 10X. Panels D were taken at 63X. (A) NIF mouse. (B,C) IF mouse section that shows ventral lateral meningitis on the left and right side. Also, Dorsal lateral meningitis on right side. (D) High mag of (C) showing microgliosis in the left ventral gray matter and degenerated neurons. (E,F) Inflammatory infiltration of the meninges, perivascular cuffing, and microgliosis.

The development of paralytic disease caused by several routes of inoculated Theiler's virus GDVII was investigated using susceptible mice. The incidence of paralysis and the anatomical location of paralysis corresponded to the different routes of injection with GDVII Theiler's virus (Table 1). Bilateral and/or contralateral paralysis was observed following the intramuscular, intravenous, intraperitoneal, and footpad routes of injection. All mice injected intratongue showed signs of tongue paralysis. The intracranial route of injection resulted in 100% mortality and clinical encephalitis. This data indicates that both IV and IM inoculated with TMEV can enter the CNS and replicate in neurons.

Table 1. Specificity of paralysis due to routes of injection of TMEV

Route of Injection[a]	Volume of Virus[b]	pfu injected[c]	Paralysis or Mortality[d]	Day of Paralysis[e]	Clinical Encephalitis[f]
Intramuscular	100ul	10^6 pfu	URLP/BRLP paralysis	2-4	0
Intragastric	100ul	10^6 pfu	0%	0	0
Intravenous	100ul	10^6 pfu	Fore/rear limb paralysis 80%	6	0
Intraperitoneal	100ul	10^6 pfu	Fore/rear limb paralysis 100%	6	0
Intratongue	100ul	10^6 pfu	Tongue paralysis 100%	4	0
Intracranial	10ul	10^5 pfu	No paralysis 100% Mortality	0	100%
Footpad	100ul	10^6 pfu	Fore/rear limb paralysis 100%	2-4	0

[a] The route of injection of TMEV in CBA mice.
[b] The amount of virus injected.
[c] pfu injected
[d] The incidence of paralysis or mortality observed in mice. URLP represents unilateral rear limb paralysis and BRLP represents bilateral rear limb paralysis. The percentage of mortality was only recognized in 100% of the mice injected via the intracranial route.
[e] The onset of paralysis in CBA mice.
[f] The percentage of mice that suffered from encephalitis.

Clinical observations of gastrocnemius injection with TMEV

Experimental evidence indicated a possibility of CNS invasion of TMEV by infection of skeletal muscle followed by entry of the virus via peripheral neural routes. Mice injected with GDVII Theiler's virus into the left gastrocnemius muscle showed flaccid limb paralysis between days 5 – 6 p.i. similar to poliomyelitis in humans. The initial state of paralysis was observed in the injected rear limb. Most mice showed weakness of the injected rear limb by day 3 and 4 p.i. A corresponding weakening of the contralateral rear limb was evident in 100% of mice that initially showed paralysis in the left gastrocnemius muscle with GDVII virus. Weakening of the contralateral rear limb was evident on day 5 and 6 p.i. Contralateral paralysis was not evident at the end of day 6 p.i., however, the mice were not allowed to live past day 6 p.i. It is likely that a contralateral paralysis have been clinically observed on days 7 and 8 p.i. The results indicated that the spread of GDVII virus may occur from the periphery to the inferior spinal cord. It is postulated that the virus then travels along interneurons where it then crosses over to the contralateral limb. If this paralysis were allowed to progress, it is postulated a complete contralateral rear limb paralysis would likely have developed by 7 or 8 p.i. (Table 2).

Table 2. Percentage of mice with clinical signs in IM injections

Day	No Clinical[a] Signs	Functional Loss[b] of Left Limb	Left Limb[c] Paralysis	Functional Loss[d] of Right Limb	Right Limb[e] Paralysis
1	100	0	0	-	0
2	100	0	0	-	0
3	50	50	0	-	0
4	0	100	0	-	0
5	0	50	50	+	0
6	0	0	50	+	0

[a] Percentage of mice with no clinical signs
[b] Percentage of mice with functional loss of left limb
[c] Percentage of mice with left limb paralysis
[d] Percentage of mice with functional loss of right limb
[e] Percentage of mice with right limb paralysis

Effect of TMEV infection on sciatic nerve

The average of 2-4 toe spread in the left hind limb on days 1 and 2 pre-infection for the non infected group and the GDVII infected group was 6.3 mm (See materials and method for sciatic nerve model description). The average toe spread of 2-4 in the left hind limb in the non-infected group remained at an average of 6 mm for the duration of the experiment. The initial average width of 2-4 toe spread in the left hind limb of the GDVII infected group was 5.3 mm on day 1 p.i. This average toe spread declined from 5.3 mm to 4.8 mm from day 1 p.i. to day 2p.i. There was a slight incline from day 2 to 3 p.i. to 5.2 mm. This is probably due to the time required for full recovery from anesthesia and surgery. However, there was a steady decline in the width of 2-4 toe spread by day 4 p.i. and 5 p.i. The average width was 4.8 mm. The width continued to drop by day 6p.i. to 4.2 mm (Fig. 3(A)).

The average of 2-4 toe spread in the right hind limb days 1 and 2 pre-infection for the non infected group and the GDVII infected group was 6.3 mm. The average 2-4 toe spread in the left hind limb in the non-infected group was 6 mm p.i, and it remained at this average for the duration of the experiment. The initial average of 2-4 toe spread in the right hind limb of the GDVII infected group was 5.2 mm day 1 p.i. The average 2-4 toe spread in the GDVII infected group was 5.2 mm from day 1 p.i. to day 5 p.i. Between day 5 p.i. and day 6 p.i. the width declined to 4.7 mm (Fig. 3(B)).

The initial average width of 1-5 toe spread in the left hind limb of the non-infected group, and the GDVII infected group was 9.9 mm days 1 and 2 pre-infection. In the left hind limb of the GDVII infected group the average 1-5 toe spread declined to an average of 9.1mm day 1 p.i. and day 2p.i. Between days 2 and 4 p.i. the width of 1-5 toe spread remained at 9.1 mm. There was a steady decline in the width from day 4 p.i. and day 6 p.i. The width of 1-5 toe spread was 8 mm at day 6 (Fig. 4(A)). The average 1-5 toe spread in the non-infected group remained at 9.5 mm throughout the experiment.

The average 1-5 toe spread in the right hind limb of the non-infected group, and the GDVII infected group days1 and 2 pre infection was 9.9 mm. In the right hind limb of the GDVII infected group the toe spread declined to an average of 9.1 mm day 1 p.i. and day 2p.i. There was an incline to 9.6 mm between days 2 and 4 p.i. This is probably due to animal recovery from anesthesia and surgery. Between days 4 and 5 p.i. the width of 1-5 toe spread declined to 9.1 mm. The width continued to drop by day 6p.i. to 8.6 mm (Fig. 4(B)). The average 1-5 toe spread the right limb in the non-infected group remained at 9.5 mm the duration of the experiment.

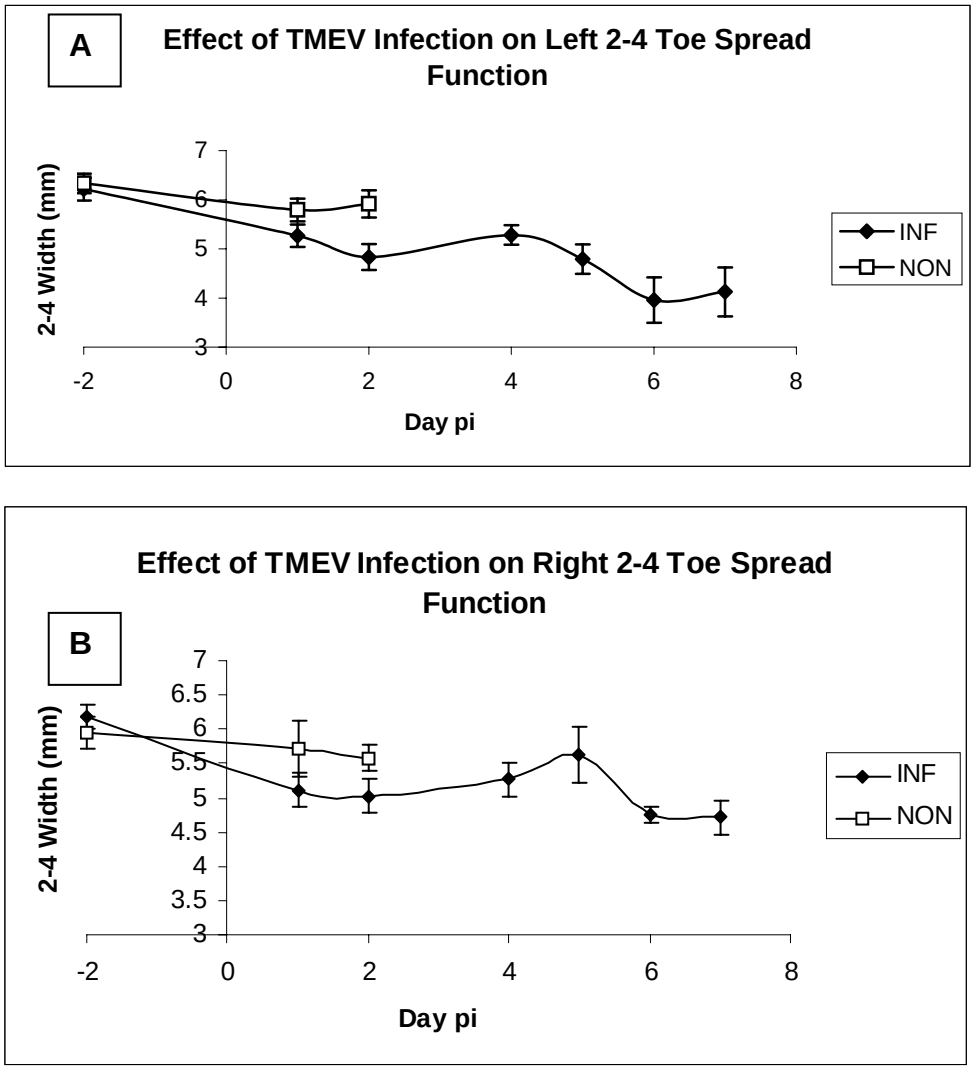

Figure 3. The effect of TMEV infection on 2-4 toe spread. (A) 2-4 toe spread on left sciatic nerve function. A steady decline in the width of 2-4 toe spread is evident by day 4 p.i. and 5 p.i. ULRLP was observed at day 5 p.i. (B) 2-4 toe spread on right sciatic nerve. A steady decline in the width of 2-4 toe spread is evident by day 5 p.i. In the time course experiment no incidence of clinical paralysis was observed in the right limb, however, contralateral rear limb paralysis was observed in the preliminary experiment (see Table 1).

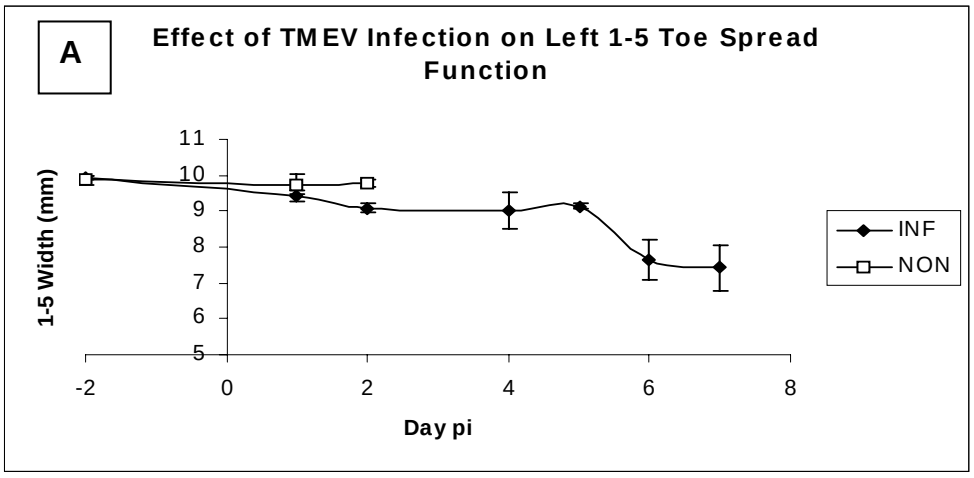

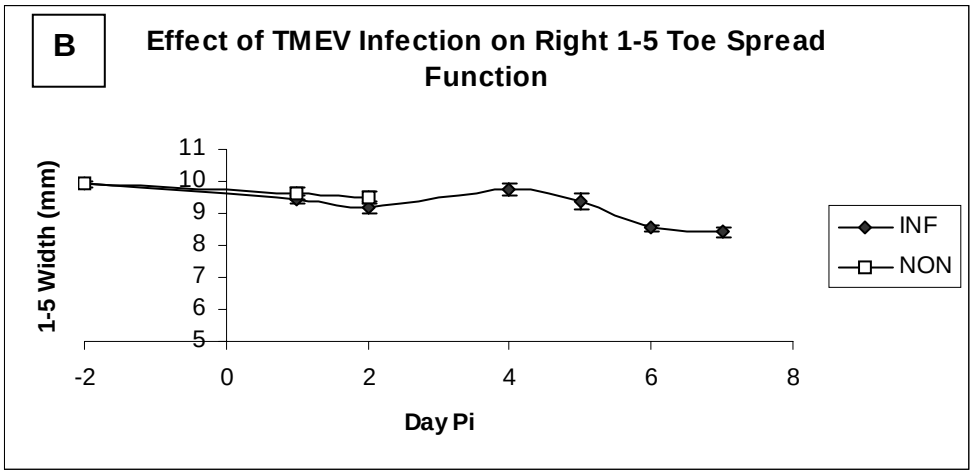

Figure 4. The effect of TMEV infection on 1-5 toe spread. (A) 1-5 toe spread on left sciatic nerve function. A steady decline begins at day 4 - 5 p.i. The incidence of paralysis was observed in the left limb at day 5 p.i. (B) 1-5 toe spread on the right sciatic nerve. A steady decline begins at day 5 p.i.

Immunofluorescence results of the gastrocnemius muscle with TMEV

Immunofluorescence was used to detect the neurotransmission of Theiler's virus from the gastrocnemius muscle, to the sciatic nerve, spinal cord, and brain following intramuscular injection of Theiler's virus. Viral antigen was detected in the gastrocnemius muscle, sciatic nerve, in the lumbar and cervical spinal cords. No viral antigen was detected in the brain.

Viral antigen was detected in the left gastrocnemius muscle on days 1 and 2 p.i. using purified rabbit anti-TMEV antibody by immunofluorescence staining (Fig. 5). The non-infected group and the infected group incubated with the secondary antibody demonstrated little to no signal (Fig. 5(A, B)). Similar results were detected with the isotype controls and infected mice (Fig. 5(C, D)). Due to the high background signal of the anti-TMEV antibody and the isotype antibody it was difficult to identify the virus in any muscle cells of the infected TMEV mice. The virus was injected directly into the gastrocnemius muscle, therefore, it can be concluded that the virus was present in the muscle, but the exact localization of the virus is inconclusive.

Viral antigen was detected in the sciatic nerve on days 2 and 3 p.i. using purified rabbit anti-TMEV antibody by immunofluorescence staining. The non-infected group incubated with the purified rabbit anti-TMEV antibody and the infected group incubated with the secondary antibody only demonstrated little to no signal (Fig. 6(A ,B)). Viral antigen was detected in the left sciatic nerves in three of the 4 mice sacrificed day 2 p.i (Fig 6(E)). At day 2 and 3 p.i. viral antigen was isolated in immune cells of the sciatic nerve (Fig 6(C, D, F)).

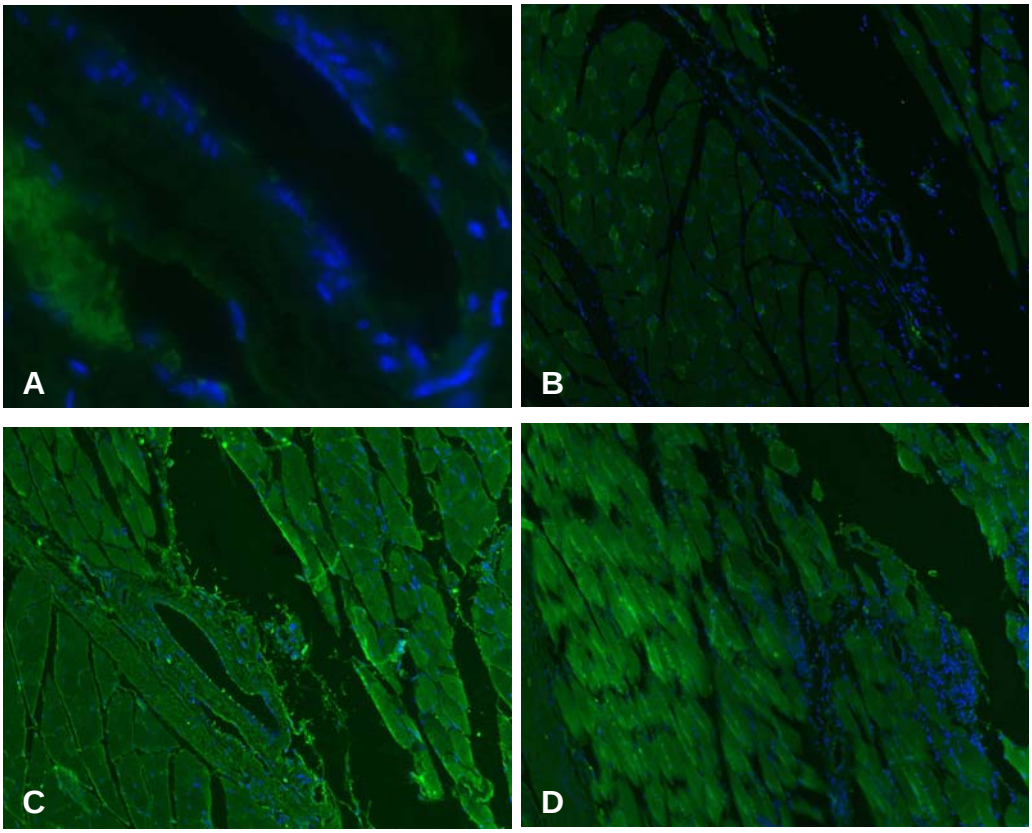

Figure 5. Immunofluorescent photomicrographs of cross sections illustrating left gastrocnemius muscle (GM) labeling. The FITC fluorochrome is the green color observed that is used for GDVII labeling. The DAPI fluorochrome is the blue color observed that is used for nuclei labeling. Panel A was taken at 40X. Panels B,C,D were taken at 10X. (A) Labeled RBC in a non-infected (NIF) mouse incubated with anti-TMEV. (B) GDVII infected (IF) mouse incubated with secondary control only. (C) GDVII IF mouse incubated with isotype control. (D) GDVII IF incubated with anti TMEV. Note that the staining patterns are different in (C) compared to (D), however, the exact location of antigen was not localized in the infected muscle sections incubated with purified anti-TMEV.

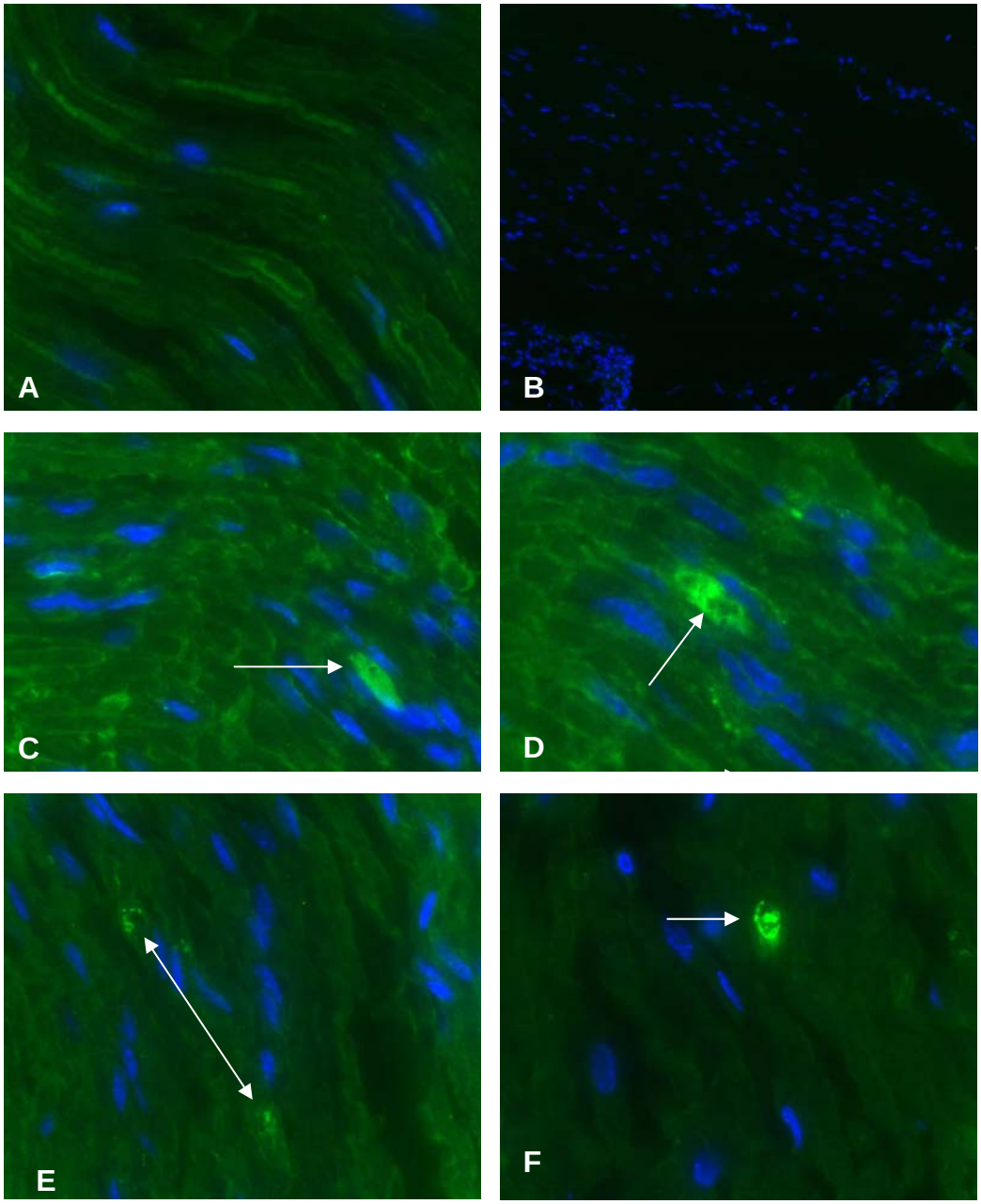

Figure 6. Immunofluorescent photomicrographs of cross sections illustrating left sciatic nerve labeling. Panels A,C,D,E, & F were taken at 40X. Panel B was taken at 10X. (A) NIF mouse incubated with anti TMEV. (B) GDVII IF incubated with secondary antibody only. (C, D) GDVII IF section incubated with anti TMEV. (C,D) Arrows point at viral antigen possibly isolated in immune cells day 2 and 3 p.i. In panel (C) the labeling appears to be localized outside the axons. In panel (D) the labeling appears to be localized in the axon. (E) GDVII IF section incubated with anti TMEV. Arrow points at viral antigen in axons. (F) GDVII IF section incubated with anti TMEV Day 3 p.i. Arrow is pointing at antigen labeling possibly localized in the axon.

A high background signal was seen in the isotype control (data not shown). The fluorescent patterns seen in the isotype control were different than GDVII infected mice incubated with purified rabbit anti-TMEV antibody. Therefore, localization of viral antigen was possible.

Uptake of Theiler's virus at motor nerve endings was confirmed by the detection of Theiler's virus antigen in the left ventral horn neurons in the lumbar section of the spinal cord at day 3 p.i. (data not shown). No staining patterns were seen in the isotype controls, secondary controls, and the non-infected mice (Figure 7 (A,B,C,)). Viral antigen in the lumbar section was detected in the left limb of mice injected with Theiler's virus. Clinical observations of mice by day 3 p.i. showed evidence of a weakening of the inoculated limb, but not complete paralysis. As clinical weakening of the ipsilateral limb progressed to the right limb, viral antigen was detected in the left side of the ventral lumbar spinal cord and also identified along the interneurons where it then crossed over to the contralateral rear limb and was detected in the right side of the ventral horn neurons of the spinal cord (Fig 7 (D,E)). The neurotransmission of viral antigen was detected in the lumbar sections of 2 out of the 4 mice sacrificed on days 3 p.i. No viral antigen was detected in the cervical or thoracic sections of the spinal cord in any of the mice sacrificed on day 3 p.i.

In the thoracic sections on days 4 and 5 p.i. viral positive neurons were identified, however not to the extent seen in the lumbar and cervical sections (data not shown). Viral antigen was detected in the lower cervical spinal cord on days 5 and 6 p.i. using purified rabbit anti - TMEV antibody by immunofluorescence staining.

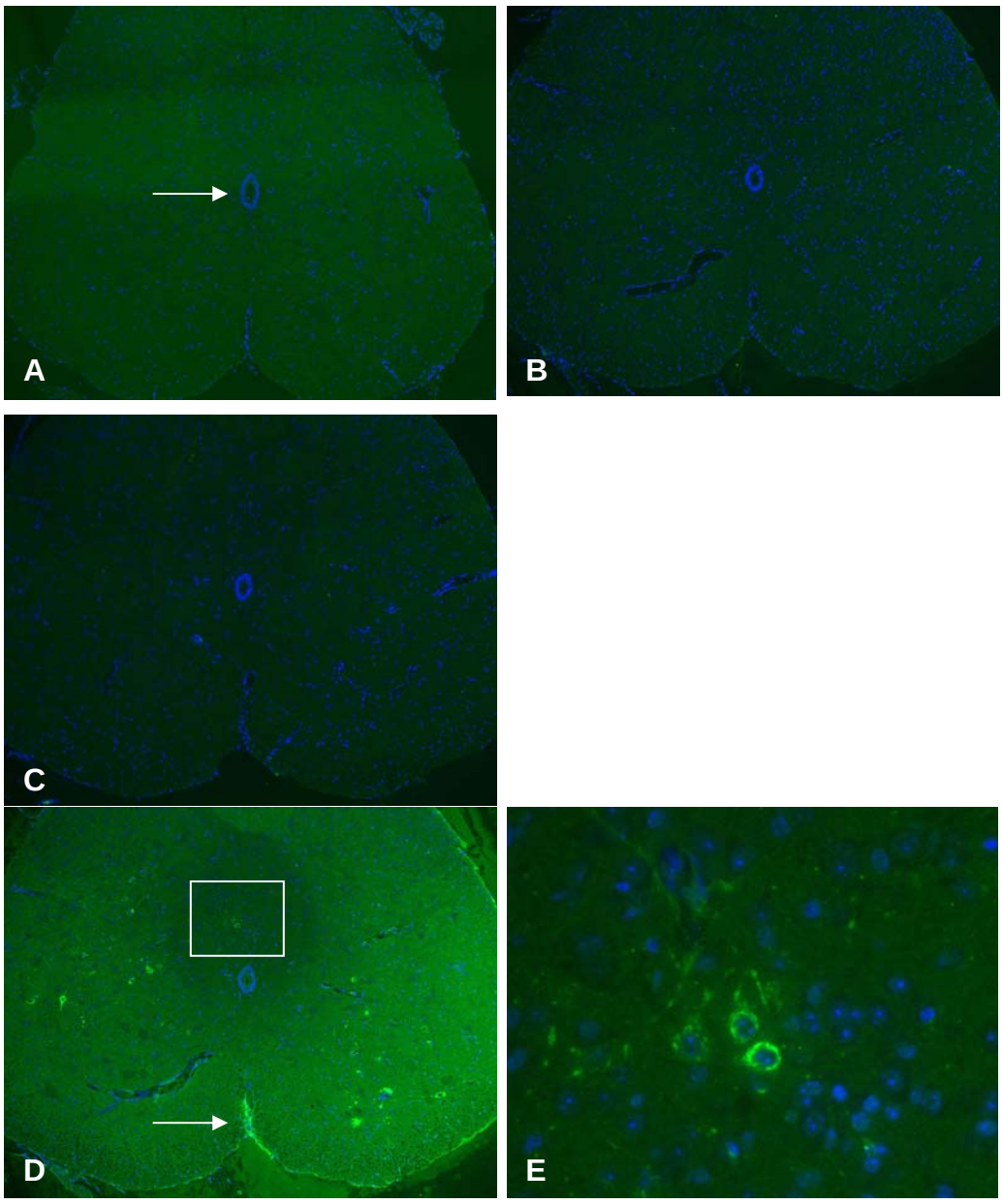

Figure 7. Immunofluorescent photomicrographs of cross sections illustrating lumbar spinal cord labeling. Panels A,B,C, & D were taken at 10X. Panel E was taken at 63X. (A) NIF mouse incubated with anti TMEV. The arrow points at the spinal canal. (B) GDVII IF incubated with secondary antibody only. (C) GDVII IF section incubated with isotype control. (D) GDVII IF incubated with anti TMEV. Viral labeling is evident in the left lumbar section and in the right ventral grey column were the lower motor neurons are located. The arrow is pointing at unspecific labeling along the ventral median fissure. (E) The insert is a higher magnification of viral antigen staining in cytoplasm of interneurons.

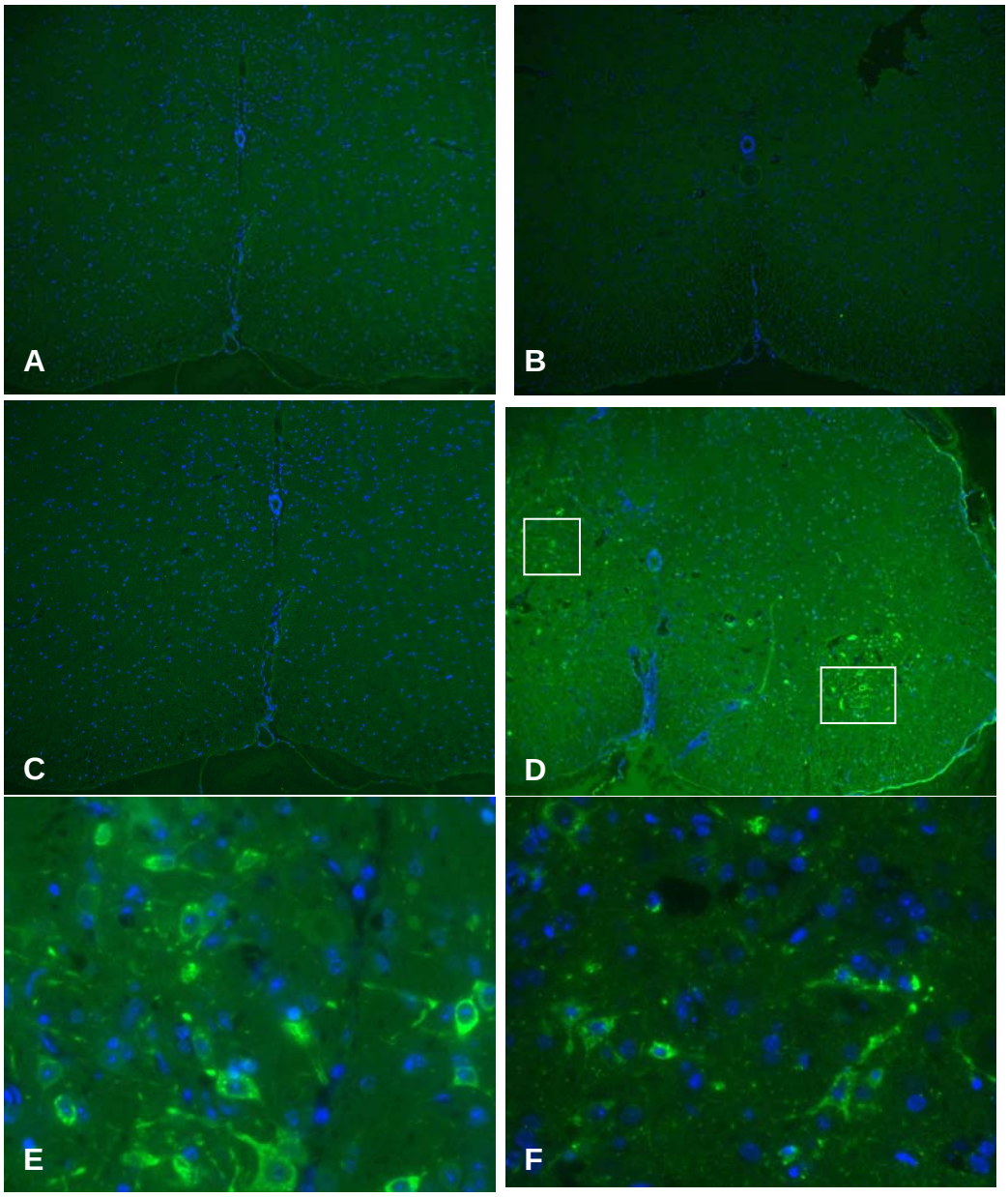

Figure 8. Immunofluorescent photomicrographs of cross sections illustrating cervical spinal cord labeling. Panels A,B,C, & D were taken at 10X. Panel E & F were taken at 63X. (A) NIF mouse incubated with anti TMEV. (B) GDVII IF incubated with secondary antibody only. (C) GDVII IF section incubated with isotype control. (D) GDVII IF incubated with anti TMEV. (E, F) Insert is higher magnification of viral antigen staining in cytoplasm of neurons.

No staining patterns were seen in the isotype controls, secondary controls, and the non-infected mice (Fig 8 (A, B, C)). Like those of the lumbar section, viral antigen was detected in the left side of the ventral lumbar spinal cord. Viral antigen was also detected on the left side of the dorsal cervical spinal cord (Fig 8 (D, E)). However, viral antigen was identified in the interneurons, where it was concluded to have crossed over to the contralateral right rear limb, and was detected in the right side of the ventral horn neurons and not the dorsal horn neurons (Fig 8 (F)). Viral antigen was detected in the cervical sections of 1 out of the 4 mice sacrificed days 6 p.i. No viral antigen was detected in the lumbar or thoracic sections of the spinal cord in any of the mice sacrificed on day 6 p.i.

The motor neurons in the ventral horn neurons of spinal cord were the prominent cells that showed fluorescence in the lumbar spinal cord sections. The viral antigen detected in the neurons was confined to the cytoplasm of the neurons. No staining was identified in the nucleus of the neurons. In the lumbar sections the localization of the fluorescence was related to the clinical signs of weakening or paralysis of the injected limb or contralateral limb, respectively. Fluorescence was also evident in the cervical regions of the spinal cord; however, no weakening of the fore limbs was evident. One explanation is that the mice were sacrificed by day 6, and not allowed to progress to full clinical paralysis. Results of the sciatic nerve model indicated a functional loss of the right hind limb at day 5 and 6 p.i.

H&E results of the gastrocnemius muscle with TMEV

Histopathological review was performed following the intramuscular route of injection with GDVII Theiler's virus. Following the intramuscular route of injection H&E stained sections of the gastrocnemius muscle, sciatic nerve, spinal cord, and brain were observed. Upon histological examination a varying severity of inflammatory cells were present between different days post-infection. The types of cells present in the gastrocnemius muscle ranged from cells of the innate immune response and acquired immune response. The cells mainly observed were monocytes/macrophages based on their characteristic morphology. Natural killer cells and mast cells were suspected to be present, however, they were not positively identified. To a lesser extent scattered neutrophils were observed, however these were mainly confined to days 1 and 2 p.i. Similar to the gastrocnemius muscle, mast cells, natural killer cells, and monocytes/macrophages were observed in the sciatic nerve. The lesions present in the CNS included mononuclear cell infiltrates and perivascular cuffs. The extent of neuronal destruction was consistent with the severity of rear limb paralysis and weakening of the contralateral rear limbs.

On day 1 p.i. of the gastrocnemius muscle a few immune cells were spread throughout the muscle (Fig. 9 (A)). By day 2 p.i. a significant amount of mononuclear cell infiltrates were observed throughout the muscle (Fig. 9 (B,C,D)). A few cells were also isolated in the connective tissue. The immune cells were identified by their characteristic morphology. Those cells clearly identified were monocytes and a few neutrophils. By day 3 p.i. severe mononuclear cell infiltrates were evident in the

gastrocnemius muscle (Fig. 9 (E, F)). Mononuclear cells were also observed along the nerve, however, most of the immune cells were localized in the muscle (Fig. 10 (B)). By days 5, and 6 severe mononuclear cell infiltrates were evident along the connective tissue of a nerve and in the connective tissue bordering the muscle and nerve (Fig. 10 (C)). A significant number of monocytes/macrophage were seen in the muscle, and along the portions of the interstitial connective tissue between muscle bundles and a nerve attached to the muscle (Fig. 10 (D, E, F)). No inflammatory infiltrates were seen in any of the non-infected groups (Fig. 10 (A)).

In the sciatic nerve no significant amounts of inflammatory infiltrates were seen at day 1 p.i. (data not shown). Inflammatory infiltrates were observed as early as day 2 p.i. and 3 p.i. By the 4^{th} and 5^{th} day p.i. a large number of inflammatory infiltrates were identified in the sciatic nerve (Fig. 11 (B)). In addition, mast cells were also suspected to have invaded the sciatic nerve; however they were not positively identified (Fig. 12 (C)). Many cells were isolated in the connective tissue (Fig. 11 (D)). The cells, mainly identified based on their morphological appearances, were monocytes/macrophages and natural killer cells. No, inflammatory infiltrates were seen in any non-infected groups (Fig. 11 (A)).

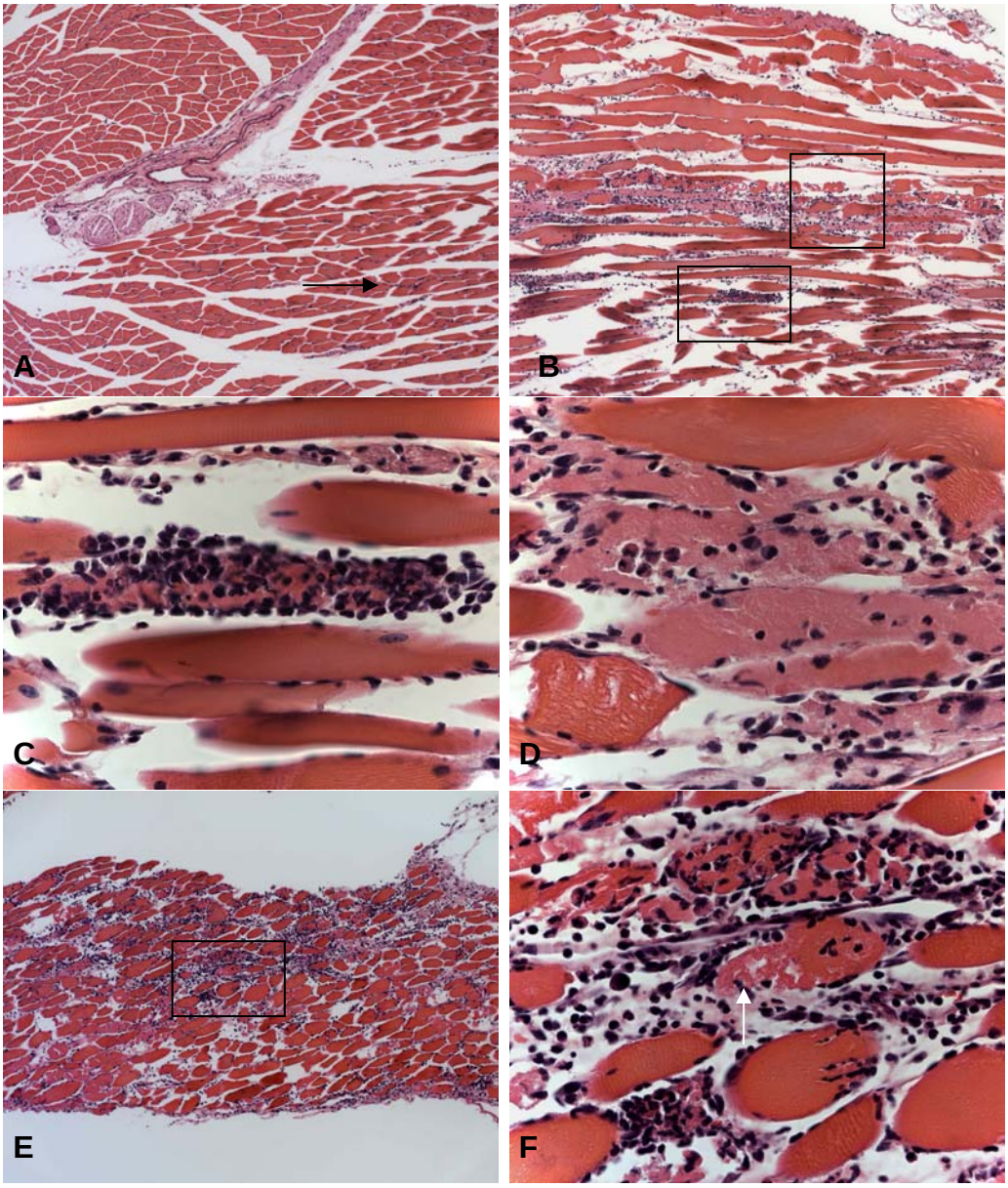

Figure 9. H&E photomicrographs of cross sections illustrating the gastrocnemius muscle (GM). Panels A, B & E were taken at 10X and panels C,D, & F were taken at 63X. (A) IF mouse GM section day 1 p.i. with little inflammatory cells. (B) Inflammatory infiltration day 2 p.i. (C,D) High mag of B of inflammatory infiltrates surrounding muscle fibers. (D) The muscle fibers are necrotic and degenerated. (E) IF mouse with severe inflammation day 3 p.i. (F) High mag. of inflammatory infiltration in the muscle. The arrow points to necrotic muscle fibers.

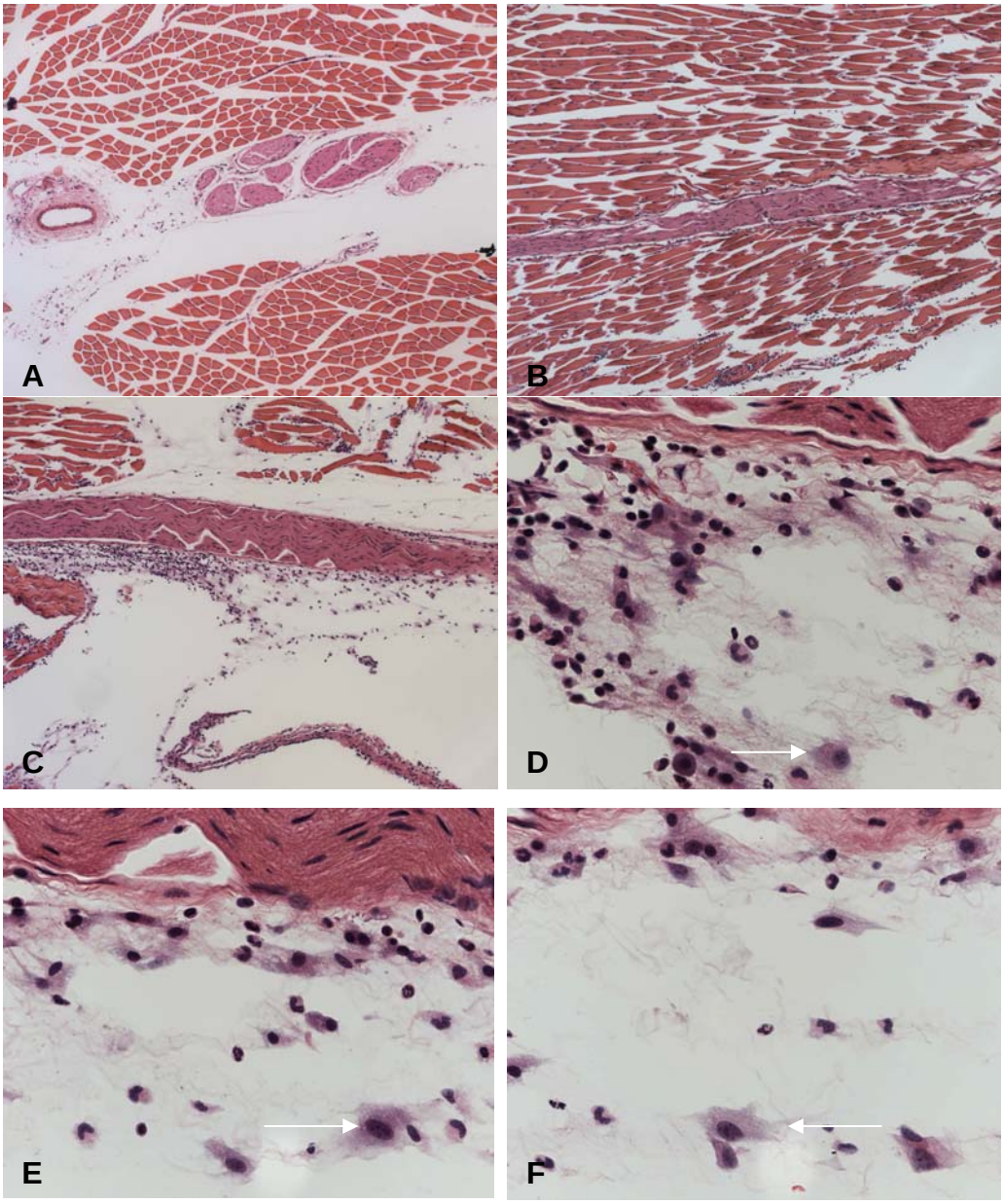

Figure 10. H&E photomicrographs of cross sections illustrating the gastrocnemius muscle. Panels A, B & C were taken at 10X. Panels D, E, & F were taken at 63X. (A) NIF mouse GM section. (B) Inflammatory infiltration along the connective tissue of a nerve at day 3 p.i. (C) Infiltration along a nerve which also affects the surrounding muscle. (D, E, F) High mag of (C) showing immune cells in the connective tissue surrounding a nerve. (D, E, F) Arrows point at macrophage in the connective tissue. Also scattered in the section are monocytes and neutrophills.

In the spinal cord no inflammatory infiltrates were evident on days 1, 2, and 3 p.i. On day 4 p.i, the animals that displayed unilateral left hind limb paralysis, showed histopathologically that there was inflammatory infiltration in the ventral side affecting the meninges in the ventral fissure (Fig. 12 (E)). Perivascular cuffs were evident in both the left and right sides of the gray matter (Fig. 12 (C,F)). Inflammatory mononuclear infiltrates were also evident in the gray matter of the left and right ventral horn in the lower lumbar segment of the spinal cord (Fig. 12 (C,D)). In addition, those mice sacrificed on day 5 p.i had a significant amount of inflammatory infiltrates and neuronal loss was evident in the cervical spinal cords (Fig. 13 (A)). The inflammatory cells invading the gray matter were found near or surrounding the neurons of the gray matter (Fig. 13 (B, E)). Inflammatory mononuclear infiltrates as well as degenerated and necrotic neurons in the gray matter of the left dorsal horn neurons and the right ventral horn neurons in the cervical segment of the spinal cord were evident (Fig. 13 (B, E)). Inflammatory infiltration was also observed in meninges of ventral fissure (Fig. 13 (D)). Perivascular cuffs were evident in the both the left dorsal gray column and the right intermediate gray column (Fig 13 (B,C)). Histopathological evaluation of mice that were sacrificed on day 6 p.i., indicated that inflammation was apparent throughout the lumbar and cervical sections of the spinal cord (data not shown). In the spinal cord meningitis was most prominent in all of the sections. Inflammatory infiltrates and perivascular cuffs were disseminated throughout the gray matter. In contrast to the immunofluorescence results, the inflammation did not appear to be confined to a specific area in spinal cord.

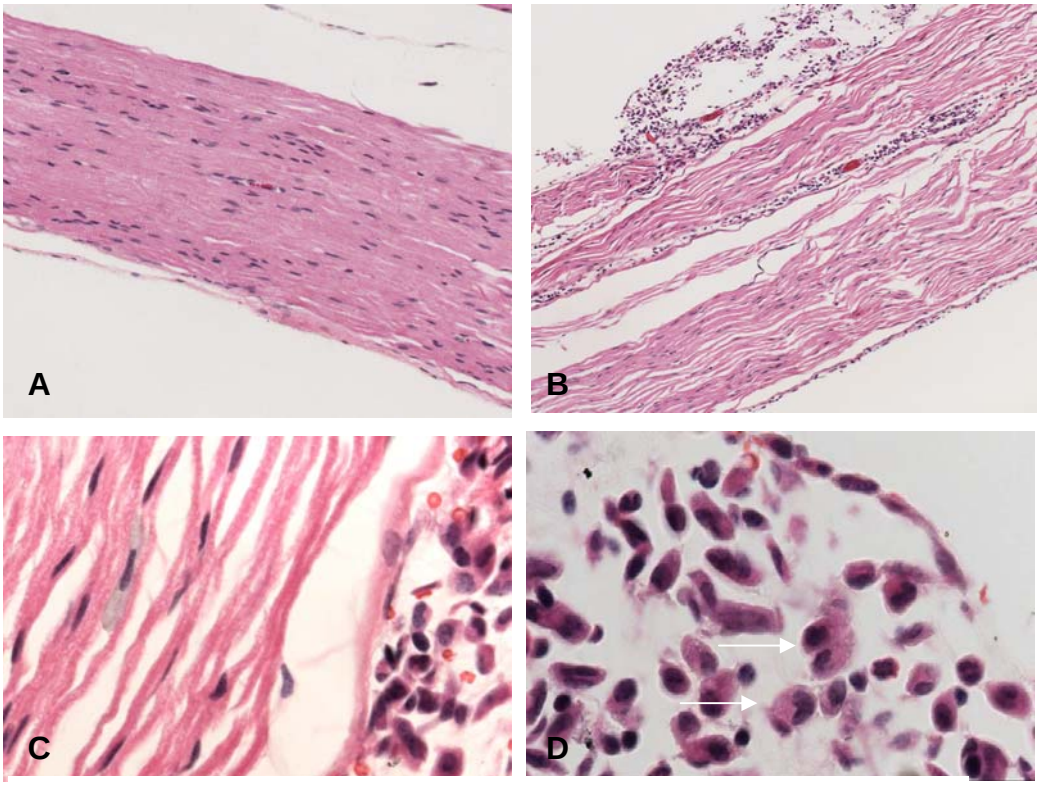

Figure 11. H&E photomicrographs of cross sections illustrating the sciatic nerve. Panels A & B was taken at 10X. Panel C&D are at 63X. (A) NIF mouse section. (B) Inflammatory infiltration of the sciatic nerve. (C) High mag of mouse section showing immune cells in the sciatic nerve. (D) Arrows point at monocyte/macrophage.

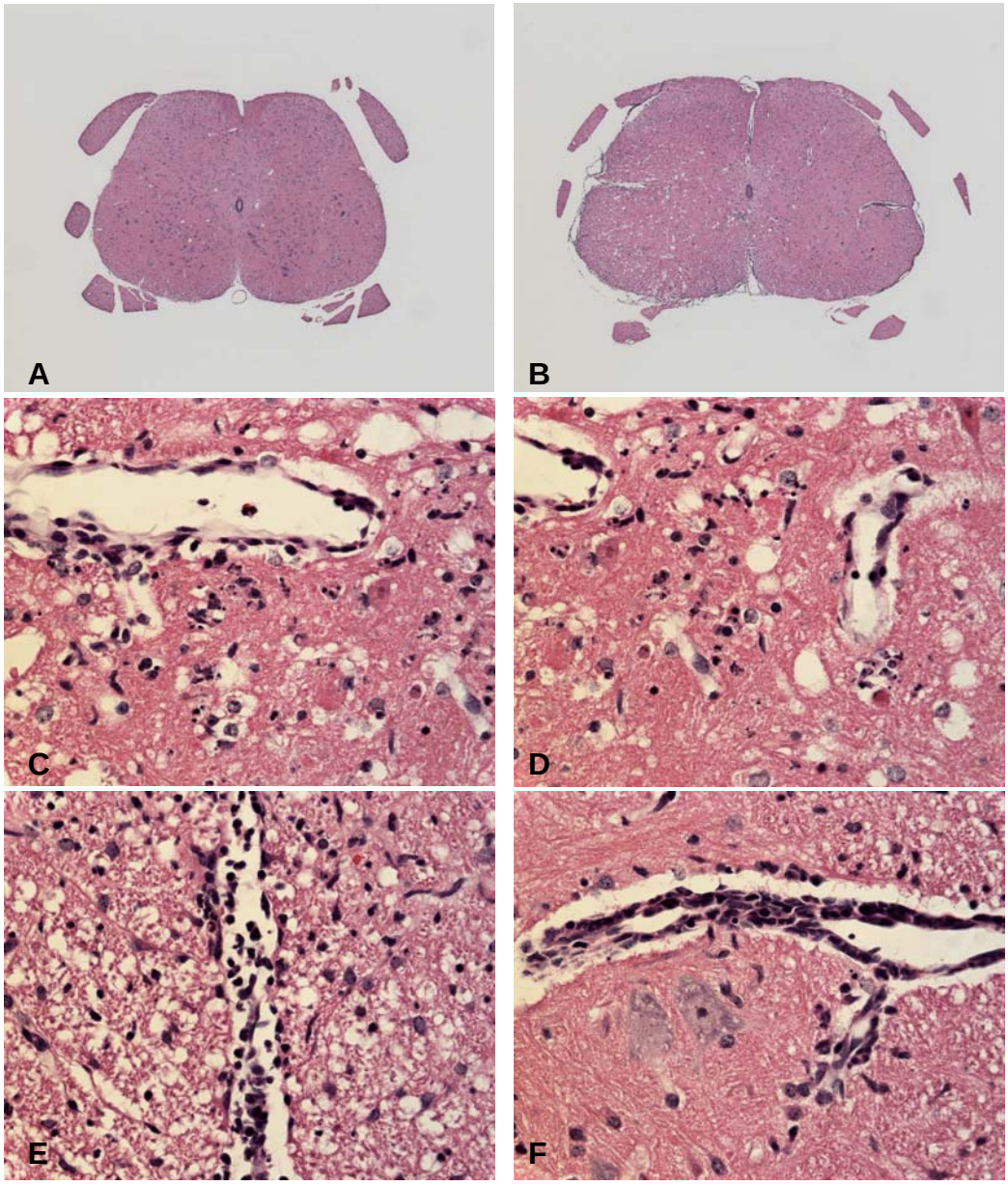

Figure 12. H&E photomicrographs of cross sections illustrating lumbar spinal cords. Panels A & B were taken at 5X. Panels C,D, E, &F were taken at 63X. (A) NIF mouse. (B) IF mouse section. (C, D) High mag of B showing perivascular cuffs and microgliosis in the left ventral gray matter. (E) Inflammatory infiltration of the meninges in the ventral fissure. (F) High magnification of B showing perivascular cuffs in the right ventral side.

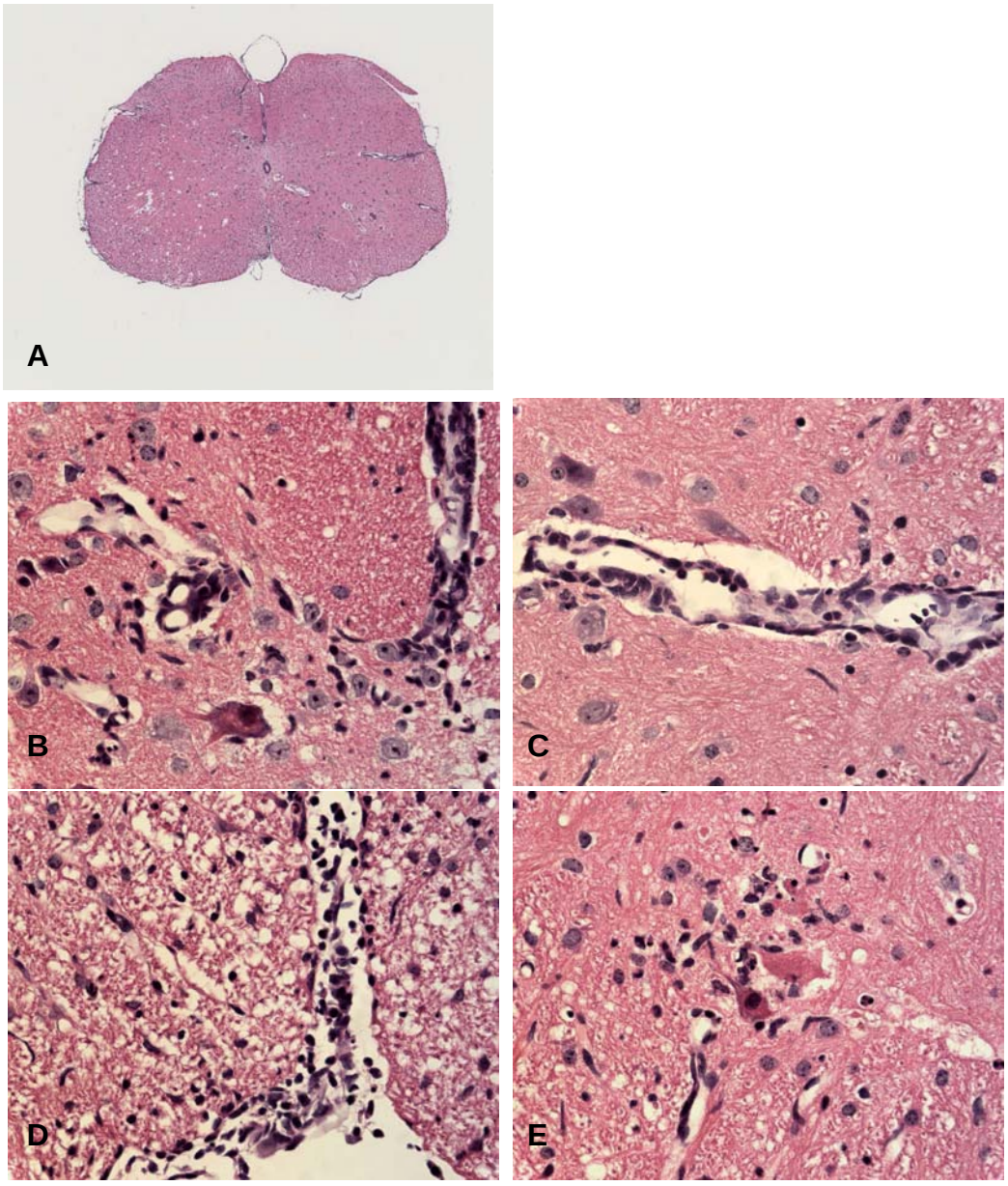

Figure 13. H&E photomicrographs of cross sections illustrating cervical spinal cords. Panel A was taken at 5X. Panel B,C, D & E were taken at 63X. (A) IF mouse section . (B) High mag of B showing perivascular cuffs in the left dorsal gray column and microgliosis of the left dorsal gray column. (C) High mag of B showing perivasuclar cuffs in the intermediate gray column. (D) Inflammatory infiltration of the meninges in the ventral fissure. (E) High magnification of B showing perivascular cuffs in the right ventral side.

Inflammation was apparent throughout the entire CNS of the mice sacrificed days 5 and 6 p.i. The clinical onset of unilateral hind limb paralysis and contralateral weakening of the right rear limb was on day 6 p.i. Perivascular cuffing, microgliosis and necrotic neurons were evident the spinal cord sections. Therefore, the severity and distribution of lesions in the spinal cord correlated with clinical disease. Paralyzed animals invariably showed inflammation and neuronal degeneration in the spinal cord.

Clinical observations of intranerve injection with TMEV

The 12th cranial nerve or hypoglossal nerve is purely a motor nerve; consequently, in this study GDVII was injected into the hypoglossal nerve (Cranial nerve XII). Experimental evidence indicates a possibility of CNS invasion of TMEV from the peripheral of CN XII by axonal transport. Mice injected with GDVII Theiler's virus into the left hypoglossal nerve displayed tongue paralysis ipsilateral to the injection site and/or a prolapsed penis. The penis of most males was prolapsed in those mice that displayed tongue paralysis, however, some of the mice displayed only tongue paralysis without a penile prolapse, and some mice suffered penile prolapse without tongue paralysis (Table 3). The disease was not allowed to progress in those mice that displayed tongue paralysis.

Table 3. Percentage of mice with clinical disease in IN injections

Day	No Clinical Signs[a]	Tongue Paralysis[b]	Penile Prolapse[c]	Both[d]
1	100	0	0	0
2	100	0	0	0
3	100	0	0	0
4	50	25	25	0
5	25	25	0	25

[a] Percentage of mice with no clinical signs
[b] Pecenage of mice with tongue paralysis only
[c] Percentage of mice penile prolapse only
[d] mice that displayed both tongue paralysis and penile prolapse

On days 1, 2 and 3 p.i. 100% of the inoculated mice appeared healthy. On day 4 p.i. 50% of the mice appeared healthy. 25% of the mice suffered tongue paralysis and the remaining two mice suffered a penile prolapse. By day 5 p.i. only one mouse displayed tongue paralysis, and the remaining two mice displayed both tongue and penile prolapse. One mouse appeared healthy on the last day p.i. Clinical observations seen in mice that displayed tongue paralysis and/or a penile prolapse were similar to clinical observations seen in mice injected intracranially with GDVII Theiler's virus (3,4, 5). Initially mice demonstrated swelling of the eyelids followed by a productive mucous discharge. As the disease progressed, mice demonstrated neck and back arching.

Immunofluorescence results of intranerve injection with TMEV

Immunofluorescence was used to detect the neurotransmission of Theiler's virus from the hypoglossal nerve, to the hypoglossal nucleus, cerebral cortex, optic nerve, other areas of the brain, and spinal cord following intranerve injection of Theiler's virus.

In the medullary areas of the brain viral antigen was detected in the hypoglossal nerve, hypoglossal nucleus, the parasympathetic nucleus of the vagus nerve, and the reticular formation lateral to the hypoglossal nucleus. In the rostral areas of the brain viral antigen was detected in the dorsal raphe nucleus. No viral antigen was detected in the cerebral cortex or the spinal cord.

No viral antigen was detected in the cervical, thoracic, lumbar, or sacral regions of the spinal cord in any of the days post infection using purified rabbit anti-TMEV antibody by immunofluorescence staining (data not shown). Results with the isotype controls and non-infected mice displayed similar results, which revealed no background staining or cross reactivity. It is postulated that the virus was not localized in the spinal cord because it could not travel from the brain to the spinal cord before the mice were sacrificed due to tongue paralysis or encephalitis.

Viral antigen was localized in the hypoglossal nucleus and neighboring neurons at day 3 p.i. (Fig. 14 (A)). The virus isolated in the hypoglossal nucleus was confined to the left hypoglossal nerve, and no viral antigen was present in the right hypoglossal nucleus (Fig. 14 (B)). Results with the isotype control, secondary control, and non-infected group contained little to no signal (Fig. 15 (A,B)). None of the signal was confined to the neurons in any of the negative controls. At day 3 p.i. viral antigen was detected in neurons of the XII nucleus on the injected side, and a few stained neurons extended to the contralateral XII nucleus (Fig 14 (C,D)). Viral antigen was seen in neurons neighboring the hypoglossal nerve and in the reticular formation (Fig 14 (E,F)). The viral antigen detected in the neurons was confined to the cytoplasm of the neurons.

No staining was identified in the nucleus of the neurons. No viral antigen was detected in the rostral area of the brain at day 1 and 2p.i or (data not shown). At day 3 p.i. and 4 p.i. viral antigen was detected in numerous neurons of both the left and right neurons of the XII nucleus (Fig. 15 (C,D)). At this stage of disease virus antigen was also detected in the dorsal motor nucleus of the vagus nerve, which is situated above the hypoglossal nucleus.

Minimal amount of labeling was evident in the metencephalon of the brain. Viral antigen was not detected in the metencephalon until the very rostral regions of this segment. Viral antigen was localized along the axons of the trigeminal nerve and along the ventral spinal cerebellar tract as well (Fig. 16 (D,E,F) . No viral antigen was detected in isotype and negative controls (Fig. 16 (A,B)). At day 4 p.i. viral antigen was detected in the medial longitudinal fasciculus, and possibly surrounding cell bodies (Fig. 17 (A,B)). At day 4 p.i. viral antigen was also isolated in the left and right neurons of the pontine reticular nucleus ipsilateral and contralateral to the injection site (Fig. 17 (C, D)). The labeling was spread out and may have affected cell bodies of the raphe magnus nucleus and the raphe pallidus nucleus. Viral antigen was also detected in the left olivary nucleus, which may have extended to the subcoeruleus nucleus (Fig. 17 (E)). No labeling was seen in the olivary nuclei contralateral to the injection site (Fig. 17 (F)). No labeling was detected in the negative and isotype controls (data not shown). No labeling was detected in the diencephalon, cerebral cortex, or optic nerve (data not shown).

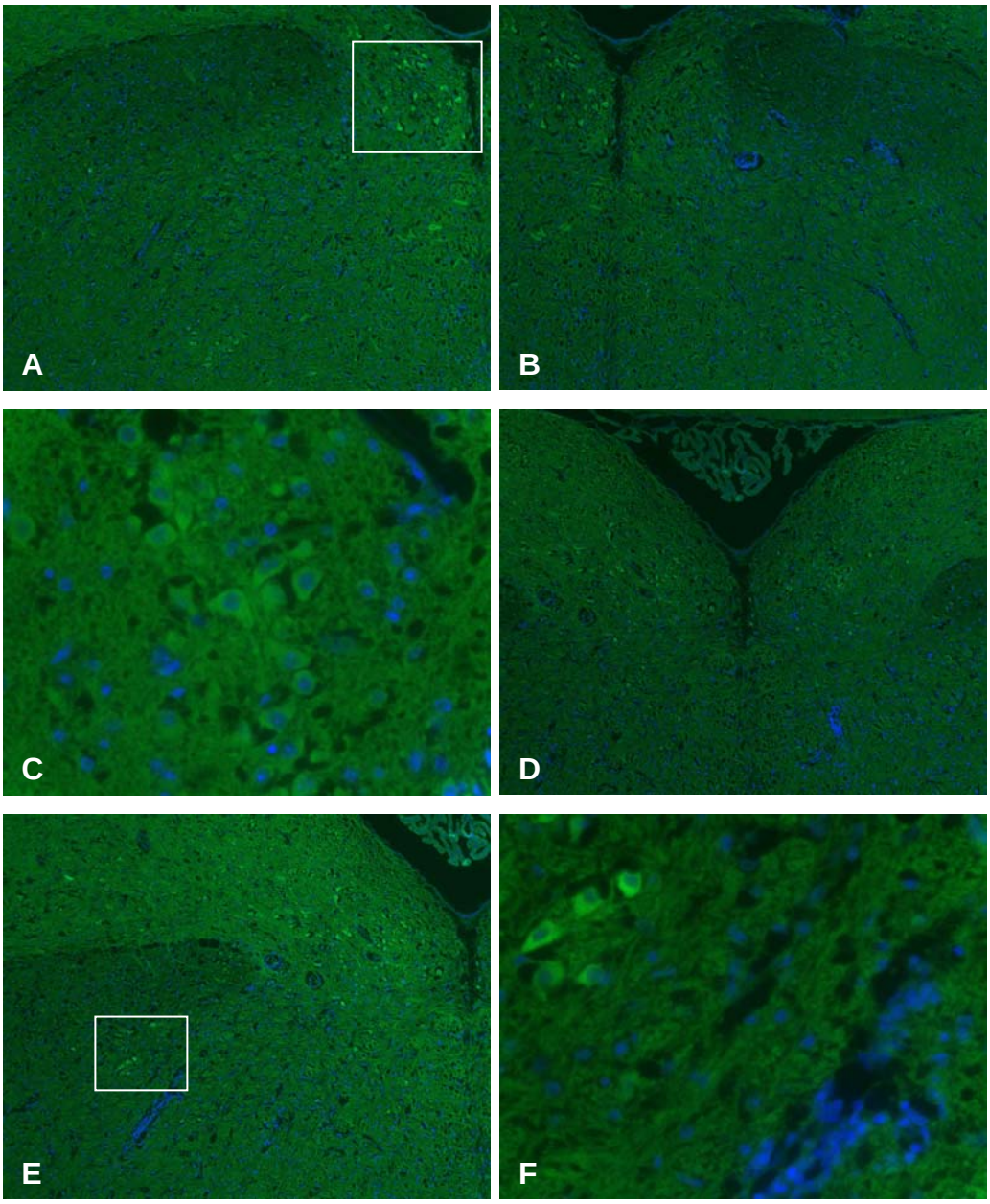

Figure 14. Immunofluorescent photomicrographs of cross sections illustrating mylencephalon labeling. Each photomicrograph shows ipsilateral labeling. Panels A,B,D, & E were taken at 10X. Panel C & F were taken at 63X. (A,B) IF mouse incubated with anti-TMEV. Labeling is confined to XII n. (C) 63X of (A) neurons and axons near the XII n. (D) GDVII IF section incubated with anti TMEV. Neurons ipsilateral and a few contralateral to inj. (D,E) GDVII IF incubated with anti TMEV. (F) Insert is higher magnification of viral antigen staining in neurons of the reticular formation.

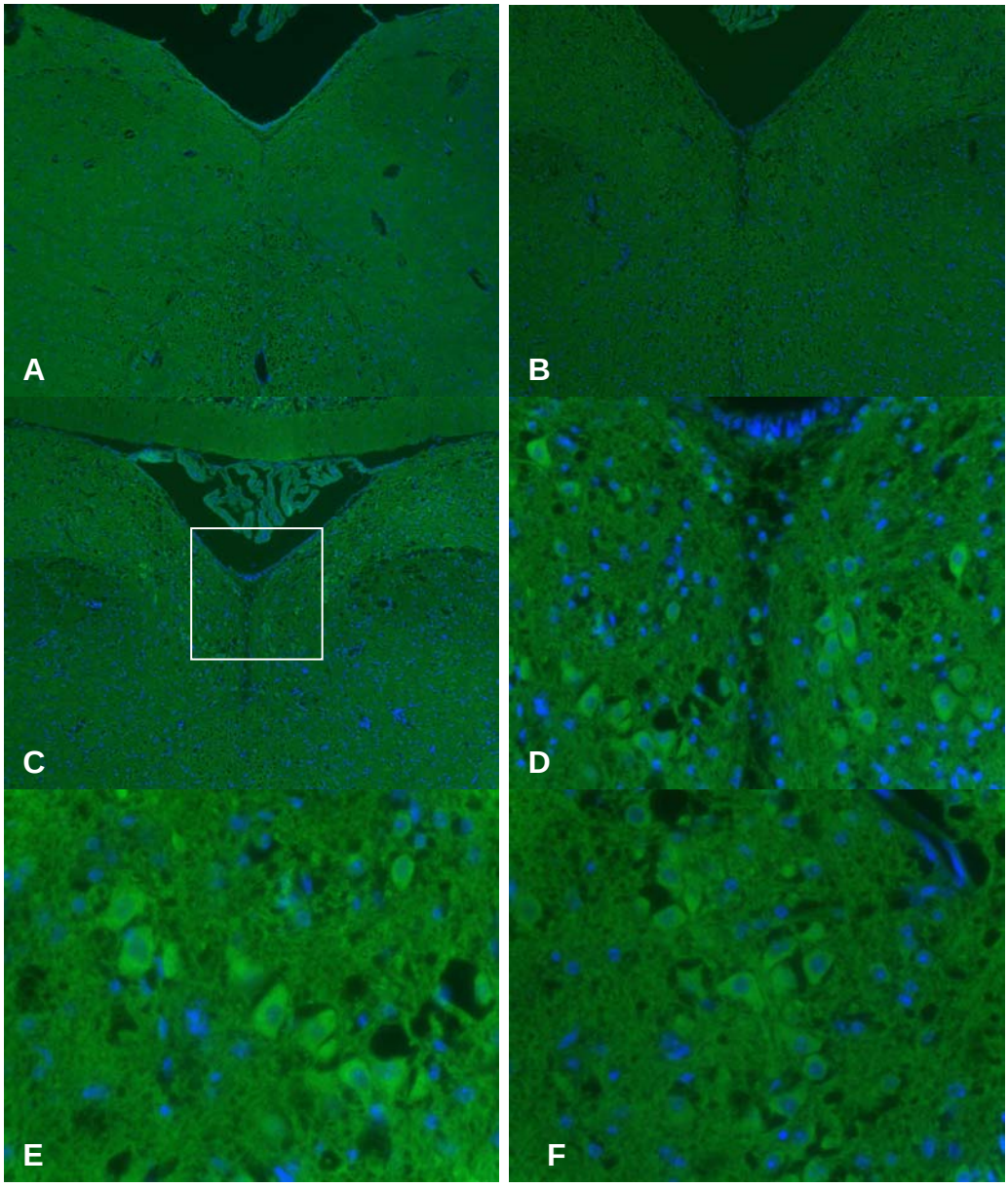

Figure 15. Immunofluorescent photomicrographs of cross sections illustrating medullary labeling. Each photomicrograph shows ipsilateral labeling. Panels A,B,& C were taken at 10X. Panel D, E, & F were taken at 63X. (A) NIF mouse incubated with anti TMEV. (B) GDVII IF incubated with isotype. (C) GDVII IF incubated with anti TMEV Neurons ipsilateral and a contralateral to inj in the XII nu. (D) 63X of C neurons in the XII n. (D) 63X of C neurons in the ipsilateral XII n. (F) 63X of C neurons in the contralateral XII n.

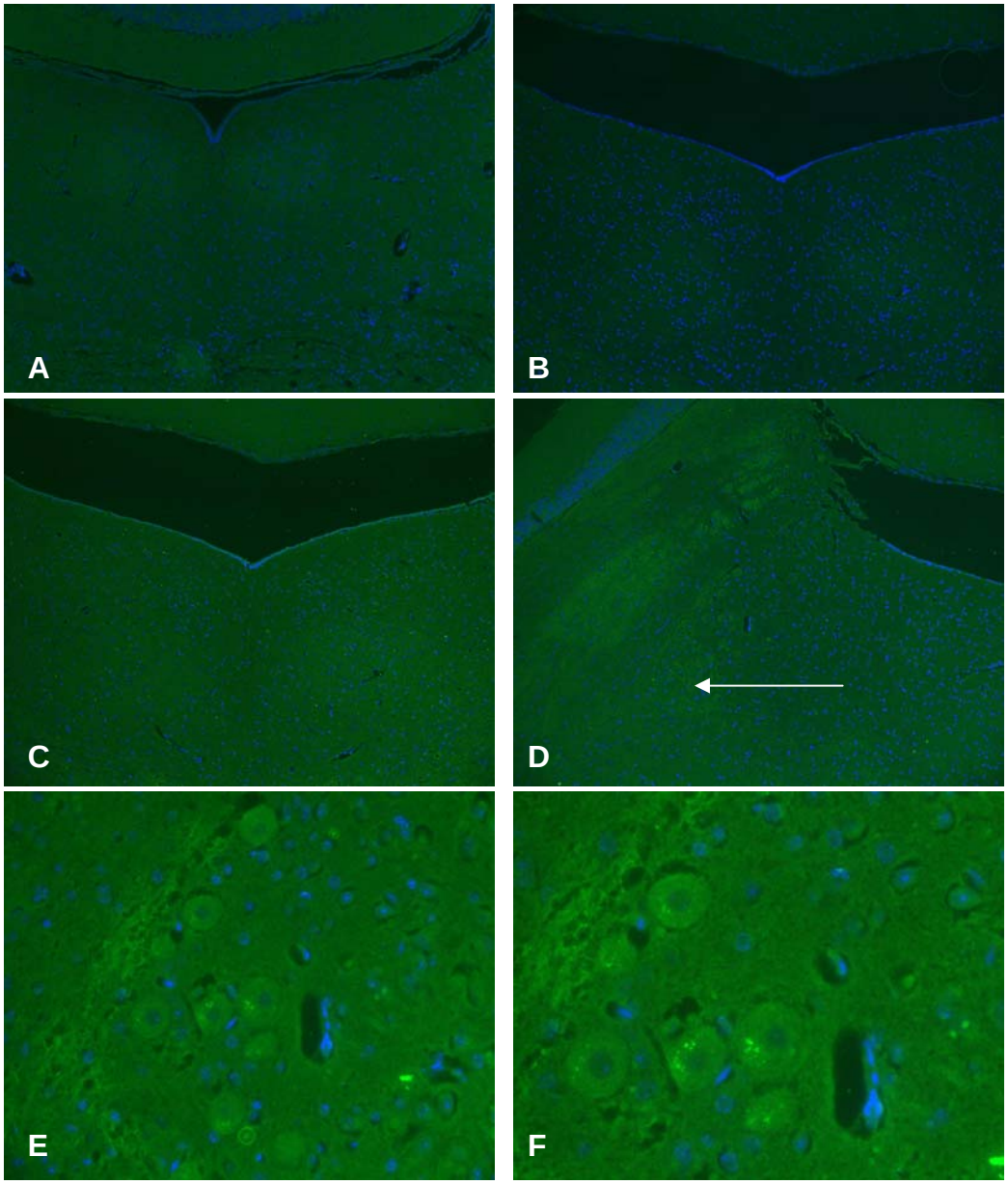

Figure 16. Immunofluorescent photomicrographs of cross sections illustrating labeling of the metencephalon. Each photmicrograph shows ipsilateral labeling. Panels A,B,C, &D were taken at 10X. Panel E was taken at 40X. Panel F was taken at 63X. (A) NIF mouse incubated with anti TMEV. (B) IF mouse incubated with isotype control. (C) IF mouse incubated with anti-TMEV with no labeling present. (D) Left view of (C) labeling in arrow points at trigeminal tracts located in this area. (E,F) High mag of (D) neurons and tracts labeled along the ventral spinal cerebellar tract and trigeminal axons.

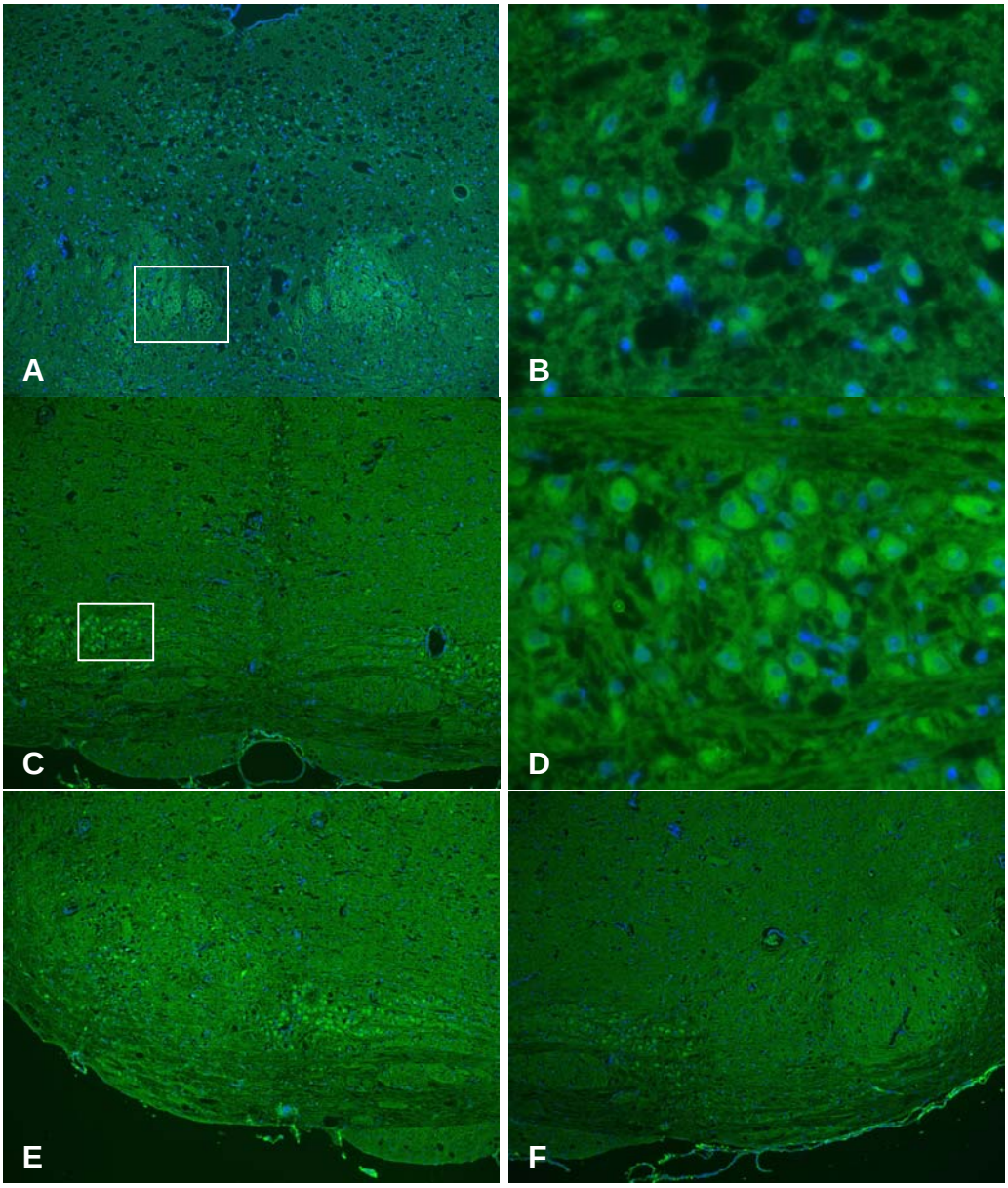

Figure 17. Immunofluorescent photomicrographs of cross sections illustrating labeling of the mesencephalon. Each photomicrograph shows ipsilateral and contralateral labeling. Panels A, C, E & F were taken at 10X. Panel B & D was taken at 63X. (A) IF mouse incubated with anti TMEV day 4 p.i. (B) High mag of A. (C) IF mouse incubated with anti TMEV day 4 p.i. possibly affecting the pontine reticular nu., raphe magnus nu., and raphe pallidus nu. located in this area. (D) Left view of C labeling of neurons (E) ipsilateral labeling arrows point to olivary nuclei and possibly affecting subcoeruleus nu. (F) contralateral view of C.

H&E results of intranerve injection with TMEV

The lesions present in the brain included presence of mononuclear cell infiltrates with and perivascular cuffing (nonsupprative encephalitis). The extent of inflammatory infiltrates was consistent with the clinical observations and immunofluorescence studies. Perivascular cuffs were seen in the hypoglossal nucleus near virally infected neurons (Fig. 18 (A,B)). Microgliosis was evident near neurons of the hypoglossal nucleus (Fig. 18 (C,D)). No, inflammatory cells were evident in the non-infected controls (Fig 19 (A)). Inflammatory infiltrates were also seen along the dorsal meninges in the mylencephalon as early as day 2 p.i., and along the dorsal meninges were viral antigen was detected in the hypoglossal nucleus (Fig. 19 (B,C)). Perivascular cuffs were seen near virus infected axons of the hypoglossal nerve ipsilateral to injection (Fig. 19 (E)). Perivascular cuffs were also seen contralateral to injection (Fig. 19 (F)). In the more rostral regions of the brain, the inflammation was seen along the dorsal and ventral meninges at days 4 (data not shown). Inflammation correlated with the immunofluorescent results. Inflammation was localized to the medial longitudinal fasciculus and surrounding cell bodies (Fig. 20 (A,B)). Inflammation was also localized in the olivary nuclei and surrounding cell bodies (Fig 20 (C,D,E, & F). No inflammation was isolated in the pontine nu. or the raphe nu. No inflammation was detected in the diencephalon, cerebral cortex, or optic nerve (data not shown).

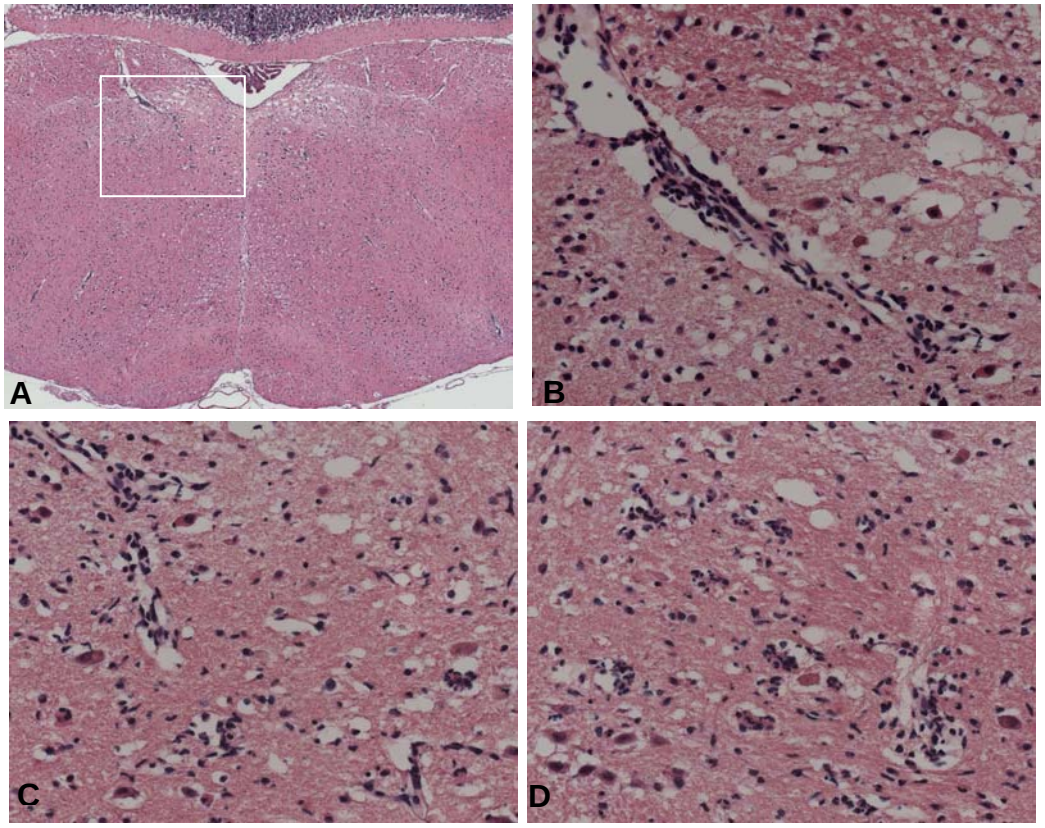

Figure 18. H&E photomicrographs of cross sections illustrating mylencephalon brain sections. Panels A was taken at 5X. Panel B, C, & D were taken at 63X (A) IF mouse section showing perivascular cuffs and inflammatory infiltrates in the ipsilateral XII nu. (B) High mag of (A) showing perivascular cuffs, microgliosis and dead neurons in the XII nu. (C,D) High mag of (A) showing presence of inflammatory cells, microgliosis, perivascular cuffing, and dead neurons of the ipsilateral hypoglossal nu.

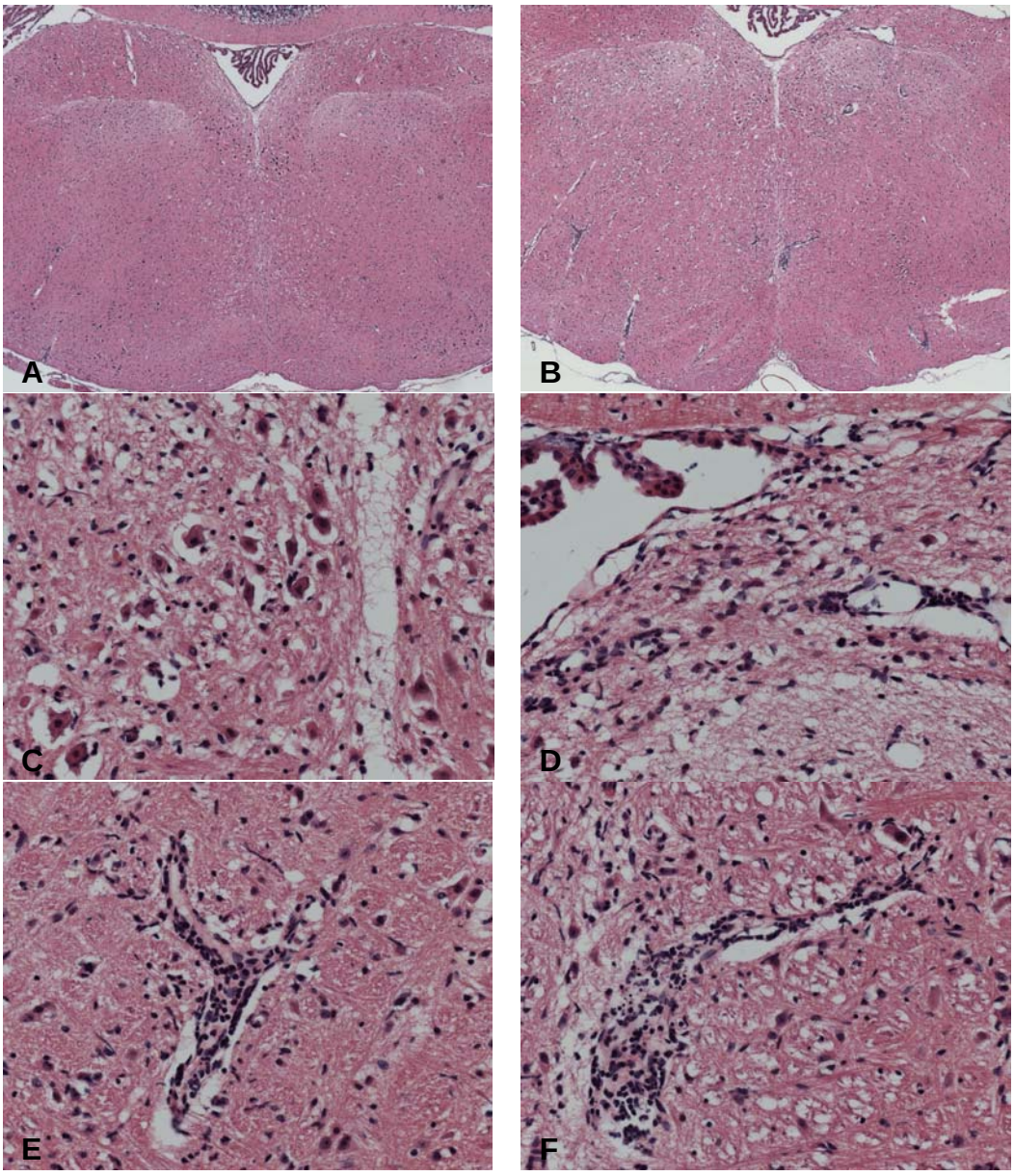

Figure 19. H&E cross sections illustrating mylencephalon brain sections. Panels A & B were taken at 5X. (A) NIF mouse section . (B) IF mouse section showing perivascular cuffs. (C) High mag of B showing microgliosis located in the ipsilateral hypoglossal nu. (D) High mag of B showing infiltration of inflammatory cells in the parasympathetic nu of X contralateral to injection. (E) Perivascular cuff ipsilateral to infection (F) Perivascular cuffing contralateral to infection.

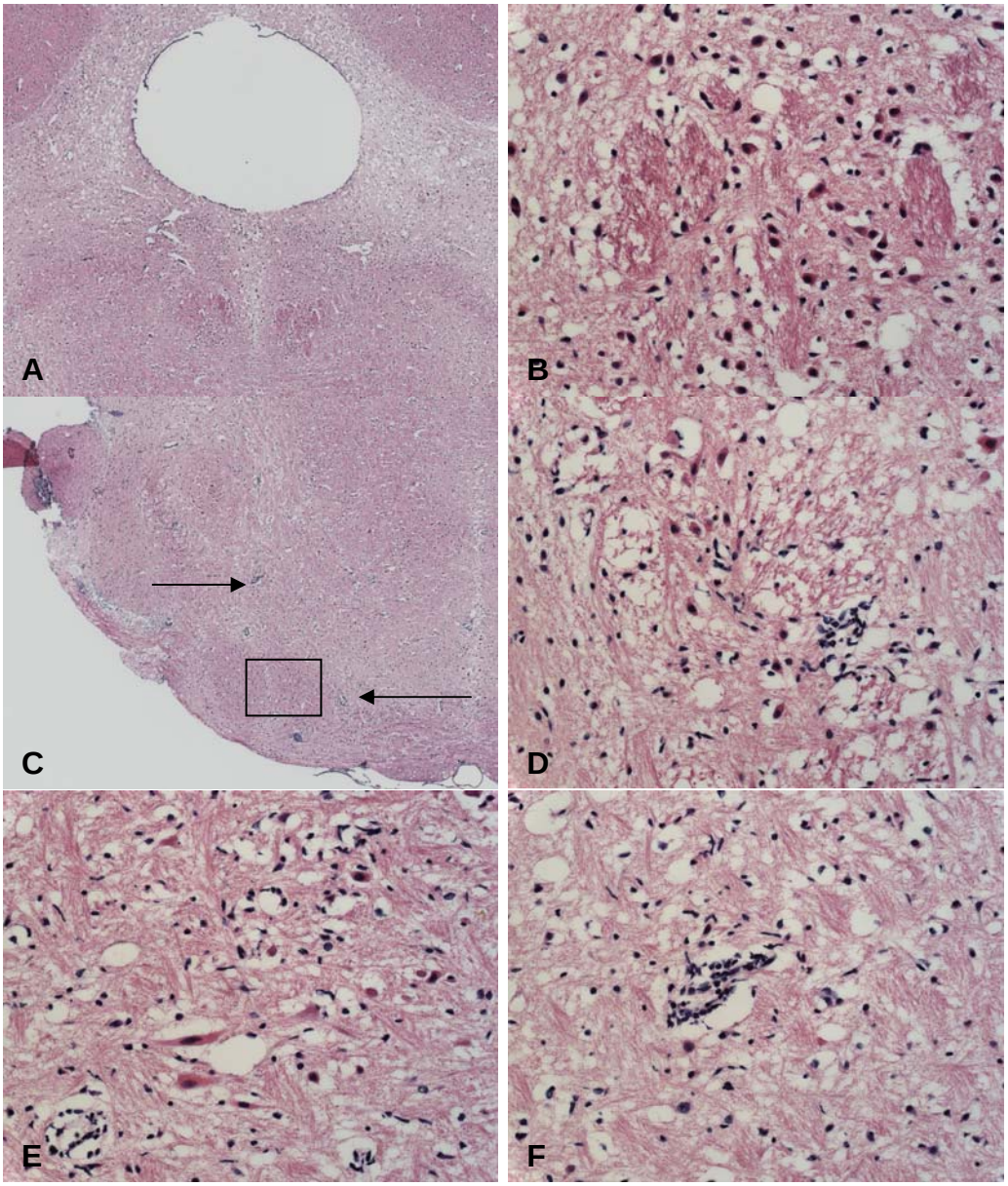

Figure 20. H&E photomicrographs of cross sections illustrating mesencephalon brain sections. Panels A & C were taken at 5X. Panels B, D, E, & F are 63X. (A) IF mouse section with inflammatory infiltrates. (B) High mag of A illustrating inflammatory infiltrates in the medial longitudinal fasciculus and surrounding cell bodies. (C) Low mag of A ventral mesencephalon. (D,E) High mag of C showing inflammatory cells, microgliosis, and dead neurons of the olivary nuclei and surrounding cell bodies ipsilateral to injection. (F) High mag of C illustrating perivascular cuffs in the cell bodies rostral to the olivary nuclei.

DISCUSSION

The development of paralytic disease caused by GDVII Theiler's virus injected into the gastrocnemius muscle was investigated using susceptible mice. The incidence of paralysis and the anatomical location of paralysis corresponded to the route of injection. Left hind limb unilateral paralysis was observed following the intramuscular route of injection. The mice showed clinical evidence of weakening of the contralateral limb. These observations correlated with the results obtained from the sciatic nerve model. In addition, the development of paralytic disease caused by GDVII Theiler's virus injected into the left hypoglossal nerve (CN XII) was investigated using susceptible mice. All mice injected in the hypoglossal nerve showed signs of tongue paralysis and/or penile prolapse. This data indicates that intramuscular and intranerve inoculated with GDVII TMEV can enter the CNS by axonal transport and infect the motor neurons of the brain and spinal cord.

It is suggested that the main viral dissemination route for GDVII Theiler's virus includes direct invasion of the CNS from the bloodstream, or by infection of peripheral organs, such as muscle, followed by viral entry from these secondary sites via peripheral neural routes. The neural pathway is not suggested to be a main viral dissemination route for intravenously inoculated virus invasion of the CNS. However, our results indicate that it may be critical in intramuscularly, intrafootpad, intratongue, and intranerve inoculated virus development of paralysis. The elaborate studies reported in the time course experiment support the concept that GDVII Theiler's virus may gain access to the CNS through a neural transport pathway. After injection of GDVII virus in the left

gastrocnemius muscle, mice exhibited left hind limb paralysis followed by weakening of the contralateral limb. In the preliminary results mice were allowed to progress to contralateral paralysis. This studies indicates that GDVII can enter the sciatic nerve via the terminal motor branches that innervate the muscle. Upon entry of GDVII into the sciatic nerve, the virus traveled in the retrograde direction to invade the lower motor neurons of the lumbar sections. Once in the CNS the virus infected interneurons, and the lower motor neurons of the contralateral hind limb. Immunohistochemical evaluation detected viral antigen in the lumbar regions of the spinal cord, interneurons, and contralateral side. The virus traveled up the spinal cord to the thoracic and cervical regions. Only a few positive neurons for viral antigens were detected in the thoracic region; however, viral antigen was detected in the cervical spinal cord. Viral antigen was specifically detected in the upper motor neurons regions, and in the interneurons crossing to the upper motor neurons of the contralatereral side.

The mechanism of entry of GDVII at nerve terminal remains unclear; however many substances that use the fast retrograde transport are thought to be packed in endosomes. Experimental evidence suggests the cytoplasmic domain of the human poliovirus receptor (hPVR) associates with Tctex-1 [34, 35]. Tctex-1 is a proven light chain of cytoplasmic dynein motor complex. It is known that the fast retrograde transport system is thought to be largely dependent on microtubules. The microtubules of the cytoskeleton serve as tracks for the movement of most membrane bounded organelles and vesicles including Golgi, endosomes, mitochondria, secretory vesicles, and synaptic vesicles. Two motor proteins of microtubules are used for the movement of

organelles from the cell center to the periphery (anterograde transport) requires kinesin, while dynein moves organelles from the periphery toward the cell center (retrograde transport) [36]. Additionally, collections of microtubules are also seen at the periphery of cells.

Rabies virus is a neurotropic virus that has been studied for its ability to spread from a peripheral site to the CNS in the retrograde direction by axonal transmission [37]. Rabies virus is a small enveloped RNA virus that is classified as a member of the Rhabdoviridae family. The direction of rabies transport into the CNS has been studied following i.c, i.m., ocular, nasal, and foot pad injections [37]. Following intramuscular injection of rabies virus, replication may occur first in the striated muscle cells. The virus will then gain access to unsheathed neural endings in motor nerve end plates, and then spread along peripheral nerves to the CNS [37].

In the intramuscular injections with TMEV the histopathological results correlated with the immunohistochemical results. In the gastrocnemius muscle the cells identified were monocytes/macrophages and natural killer cells based on their morphological appearances. These cells are seen in both the early and late immune response, and are actively involved in combating viral infection. Viral localization was not clearly identified in the gastrocnemius muscle. In spite of this, mononuclear cell infiltrates were located in the muscle and along the interstitial connective tissue located between the muscle fibers and an attached nerve. The number of immune cells along the nerve increased by the 4^{th} and 5^{th} days' p.i. In the sciatic nerve monocytes/macrophages and natural killer cells were also identified based on their morphological characteristics.

In addition mast cells were also suspected to have invaded the sciatic nerve; however they were not positively identified.

Mast cells are commonly involved in IgE-associated allergy infection, and in parasitic early immune responses [29, 38]. However, research suggests that they are actively involved in microbial infections. In the early immune response they have been shown to play a role in the host immune response against gram-negative bacteria [39]. In this study research supported evidence that mast cells can recognize and engulf bacteria. This stimulates the release of cytokines such as IL-4, IL-6, and TNF-α. These cytokines are important in the acute phase response and can trigger inflammation to respond to a bacterial infection. In addition, certain progenitors of human mast cells express CD4 [40]. CD4 cell markers have been previously identified on T-helper cells, monocytes/macrophages. These cell markers function in MHC class II responses and are also the Human Immunodeficiency Virus (HIV) receptor. HIV is a retrovirus that attacks these immune cells that contain CD4 receptors on their cell surfaces. These receptors allow entry of HIV viral RNA into the cell. Upon entry, an enzyme called reverse transcriptase will act as a template for its RNA to DNA transcription. This will allow the viral RNA to be integrated into the cells DNA. Mast cells that express CD4 markers have shown to be infected with HIV-1 strain in the blood of AIDS patients [40]. In addition, supporting research suggests mast cells can secrete IL-16 [41]. IL-16 is a chemoattractant for CD4 T-lymphocyte, and macrophage/monocytes, IL-16 also inhibits HIV viral replication [41].

The severity and distribution of lesions in the spinal cord correlated with clinical disease and the presence of TMEV viral antigen in immunohistochemical analyses. In the CNS inflammation was apparent in the lumbar, thoracic, and cervical sections of the spinal cord. The clinical onset of unilateral hind limb paralysis and contralateral weakening of the right rear limb correlated with the appearance of perivascular cuffing, lymphocyte infiltration. Microgliosis, perivascular cuffing, and neuronal destruction were evident in the grey matter. A number of necrotic cells were identified based on their morphological appearances. Apoptotic cells were not identified, however, apoptotic cells have been identified in viral infection and neurological diseases such as Multiple Sclerosis. In Theiler's virus the presence of apoptotic cells has been studied during both the acute and chronic phase of disease [42, 43, 44, 45]. Specifically, one study examined the cell types involved during the acute phase of GDVII and DA virus infection, and the chronic phase of DA virus [42]. In the acute phase apoptotic cells were located in the neurons of both brain and spinal cord with both virus infections. In the chronic phase apoptotic cells were identified in glial cells and oligodendrocytes in the white matter of the brain and spinal cord.

As previously stated, mice injected intranerve showed signs of tongue paralysis and/or penile prolapse. The hypoglossal nerve, or twelfth cranial nerve, is a somatic efferent (motor) nerve that innervates both intrinsic and extrinsic muscles of the tongue. In mice Theiler's virus causes motor deficits; consequently the results would not be interfered by neighboring sensory fibers that are connected to the same interneurons. Mice injected in the hypoglossal nerve, displayed tongue paralysis. This data suggest

that entry of GDVII Theiler's virus into the CNS is through retrograde transneuronal transport of the virus from the XII motor neurons to their premotor interneurons and thus gains access to the CNS. A number of studies have identified the hypoglossal nerve branches and the hypoglossal nucleus premotor branches using psuedorabies as transneural tracer or HRP retrograde labeling [46, 47]. Premotor braches have been identified in the parvocellular reticular formation, medullary reticular formation, the nucleus of Kölliker-Fuse, and the reticular formation around the trigeminal (V) motor nucleus [47]. In more rostral reticular formation regions of the mylencephalon, labeling was identified in the nucleus gigantocellularis, raphe pallidus, and raphe magnus [46]. In the pons or mid brain labeling was identified in the subcoeruleus nucleus and the motor trigeminal nucleus [46].

The results identified in this study were slightly different. Viral antigen was identified in the hypoglossal nerve, neurons of the XII nucleus on the injected side, and the contralateral XII nucleus, in the reticular formation lateral to the nucleus, and in the medullary reticular formation of the mylencephalon. These results correlate with HRP and psuedorabies retrograde labeling. However, in the later stages of disease viral antigen was also detected in the dorsal motor nucleus of the vagus nerve. This nucleus is situated above the hypoglossal nucleus. Viral antigen was also detected in the medial longitudinal fasciculus, which is located below the XII nucleus. This is most likely the result of neuronal destruction by the virus in adjacent surroundings not connected to the hypoglossal nucleus. Viral antigen was detected in the more rostral regions of the mid brain surrounding the trigeminal nuclei. The axons of the motor trigeminal nucleus

project to the muscles of mastication [48]. The axons of the pontine sensory nucleus of trigeminal nerve project tactile and proprioception to the face [48]. It may be difficult to evaluate any loss function due to CN 5 (trigeminal cranial nerve 5). Upon clinical examination the mice suffered a mucous discharge. This may have been the result of loss of sensation to blink or produce tears by the mouse. However, the mucous discharge could have also been a result of dehydration due to weakening of the tongue and subsequently paralysis of the tongue. A significant amount of viral antigen was detected in the mesencephalon region of the brain. Viral antigen was localized in the medial longitudinal fasciculus, which contains axons of the vestibular nuclei and the abducent nucleus that coordinate eye movements for nystagmus [49]. In the ventral portion of the mesencephalon viral antigen was detected in the neurons of the pontine reticular nucleus ipsilateral and contralateral to the injection, and possibly the raphe magnus nucleus and the raphe pallidus nucleus. It was difficult to isolate the exact boundaries of viral labeling. Viral antigen was also detected in the left olivary nucleus, which extended to the subcoeruleus nucleus. No viral antigen was detected in the diencephalons, cerebral cortex, or optic nerve. This may be due to the fact that mice suffering from tongue paralysis and encephalitis, were sacrificed before further viral dissemination could occur.

Similar studies using, Herpes simplex virus type 1 injected into the hypoglossal nerve demonstrated viral antigens in glial cells at the XII root entry zone, XII nucleus, the lateral reticular formation, Kölliker-Fuse nucleus, dorsal raphe nucleus, and nucleus coeruleus [50]. In contrast to this study no viral positive neurons were detected in the

dorsal motor nucleus of the vagus nerve, however, virally infected glial cells were located in this area. In the lateral brainstem virus positive neurons were detected before the appearance of positive glial cells, and in the lateral reticular formation neurons were positive without positive glial cells [50]. This may indicate that glial cells were infected secondarily due to infection of the neurons. These results indicated that the propagation of HSV via the hypoglossal nerve occurs mainly within the neural circuitry.

The penis of most affected males was prolapsed. Studies using pseudorabies as a transneuronal transport tracer to identify any existing CNS innervation of the penis, have demonstrated transneuronally labeled neurons in the reticular formation of the medulla, paraventricular nucleus of the hypothalamus [51]. The medullary reticular formation is located ventral to the hypoglossal nucleus. The axons of CN XII also pass through the medullary reticular formation. The medullary reticular formation contains axons for parasympathetic upper motor neuron axons to GVE LMNs in the sacral spinal cord [48]. Viral antigen was detected in the medullary reticular formation which may have caused the clinical symptoms of prolapsed penis in the mice.

The severity and distribution of lesions in the brain correlated with clinical disease and the presence of viral antigen in immunohistochemistry analyses. In the brain inflammation was apparent in the hypoglossal nerve, bilateral in the hypoglossal nucleus, and dispersed throughout the reticular formation in the medullary area. In the rostral areas of the brain microgliosis was evident near virally-infected neurons as well. Microgliosis, perivascular cuffing, and degenerated neurons were evident in the grey matter near neurons. Moreover, intense areas of perivascular cuffs were evident near

viral positive neurons. The clinical onset of tongue paralysis and penile prolapse correlated with the appearance of lymphocyte infiltration of the meningitis dorsal to affected areas.

During normal physiologic conditions there is little evidence that supports the presence of circulating lymphocytes that can migrate through endothelial cells and gain entry into the CNS [52]. However, the hematogenous entry of an infectious agent into the CNS by crossing the BBB may be due to infection and replication in endothelial cells and/or macrophages. This may stimulate undifferentiated circulating macrophages to cross the BBB and become activated by the presence of IFN-γ released by resident glia [53]. The mononuclear cells can then upregulate the expression of MHC class II and therefore activate lymphocytes. The BBB contains special structural and functional features of the brain capillaries that limit the access of materials from the blood into the brain and cerebral spinal fluid. These specialized properties of the BBB include endothelial cells and their intercellular junctions that restrict vesicular transport and protect the CNS from harmful substances circulating in the blood.

The CNS and the eye are immune privileged organs that developed in order to protect specialized tissue incapable of regeneration [53, 54]. Both have developed several mechanisms to maintain an immunologically privileged status. The BBB controls immunity by regulating the entry of lymphocytes, and macrophages into the CNS [32, 53, 54]. Few tissues in the neural-ocular system contain bone-marrow derived cells that express MHC class II molecules, and these are limited in their antigen processing and presenting capabilities [53, 54]. Moreover, the eye and brain both lack

the conventional lymphatic drainage pathway, and therefore is highly specific to which inflammatory infiltrates can enter [52, 53, 54]. Therefore these organs do not elicit the same inflammatory response seen in non-privileged sites.

In non-privileged sites pathogens will enter the body via many routes, but antigen and lymphocytes will eventually encounter each other in the peripheral lymphoid organs, which include the lymph nodes, the spleen, and associated mucosal lymphoid tissues [52]. Lymphocytes are continually present in these tissues. Antigens are carried through infected tissues, primarily within antigen presenting cells (APC), macrophages and dendritic cells. These cells are precursors from the bone marrow and express both class I and II major histocompatibility complex (MHC) molecules [52]. Naïve T cells become activated once APC process and present antigen to naïve T cells by means of the MHC class II complex or I [32, 52].

CONCLUSION

There are two possible methods of entry into the central nervous system for TMEV; first by the hematogenous route and /or secondly the neural route. Experiments for the future include similar detailed time course experiments using less virulent strains of TMEV, DA and Bean with respect to different routs of injection. With these models we hope to address the following experimental questions: 1) how do these viruses gain access to the CNS, and 2) once in the CNS how do these viruses spread?

MATERIALS AND METHODS

TMEV

The strain of GDVII Theiler's virus used throughout this study was obtained from Dr. H. L. Lipton, Department of Neurology, University of Chicago, Evanston, IL. The GDVII strain of Theiler's virus was amplified in L2 cells. The culture supernatant that contained infectious virus was aliquoted and stored at -70˚C before use [55].

Animals

4 – 6 week old male CBA strain mice were used in this study (Harlan Sprague Dawley, Inc., Indianapolis, Indiana). They were housed in a BSL II containment animal room in the Laboratory Animal Resources and Research (LARR), College of Veterinary Medicine, Texas A&M University, TX.

Animal inoculations

The mice were anesthetized with ketamine (100mg/kg) and xylazine (5mg/kg) via the intraperitoneal route. Following administration of the anesthetic, the mice were injected with GDVII strain of Theiler's virus into the intramuscular injection into the left medial gastrocnemius muscle, and intrahypoglossal nerve.

Animal surgery

Microsurgery was performed for the injection into the hypoglossal nerve and the intramuscular injection into the medial gastrocnemius muscle. For the intrahypoglossal nerve injection, a sagittal incision was made in the skin from the intramandibular space. A longitudinal incision was made over the digastric muscle and mylohoidis muscle, and they were retracted downward in order to expose the XII nerve. The nerve was carefully

abraded before the virus suspension was administered. A 34-gauge needle was inserted into the nerve, and approximately .8ul to 1ul of the virus was slowly injected into the nerve. The virus titer used was 10^8 p.f.u./ml. Special care was taken during the surgery to keep the blood supply intact in order to avoid virus exposure to the blood stream. The tissues around the nerve and the wound were then sutured. Each mouse was observed daily for any paralysis, including tongue paralysis and/or encephalitis, and sacrificed on day's one, two, three, four, five, six, and seven days post infection, respectively.

For the intramuscular injection, the mouse was depilated on the left rear limb and placed under a dissecting microscope. The skin on the ventral surface of the limb was cut along a line parallel with the gastrocnemius muscle. The gastrocnemius muscle was exposed upon removal of subcutaneous connective tissue. Similar to the nerve injection, the blood supply was kept intact in order to avoid virus exposure to the blood stream. A 27-gauge needle was used to inject 100ul of virus into the mouse. The virus titer used is 10^6 p.f.u./ml. The wound was then sutured. The mice were observed daily for paralysis and or clinical encephalitis, and sacrificed day's one, two, three, four, and five days post infection, respectively.

Sciatic nerve model

In addition to the clinical observations obtained, a separate blind experiment was performed using a sciatic nerve model that determines functional loss of the sciatic nerve. This is a well established model that measures the length of toe spread 1 - 5, and toe spread 2 - 4 [56, 57, 58]. In the lower limb the sciatic nerve divides into the tibial nerve and the peroneal nerve. As the mice progress to paralysis there is a decrease in the

width of toe spread between 1-5 and 2-4. The toe spread between 2-4 is dependent on the tibial division of the sciatic nerve. The toe spread between 1-5 is dependent on the tibial and peroneal division of the sciatic nerve. The toe spread between 1-5 and 2-4 were measured and the results were compared from injured and uninjured hind limbs. This experiment was also performed on non infected mice. Blue ink was placed on the hind limbs of GDVII infected group and the non-infected group. All mice were required to run on a white strip of paper along a column. The width of toe spread between 1-5 and 2-4 were measured for both left and right limbs in the GDVII infected group and non-infected group. The mice were measured up to 2 days prior to the infection and through the duration of the time course experiment.

Histopathology

All mice inoculated with GDVII Theiler's virus either intramuscular or intranerve were administered a lethal dose of phenobarbital intraperitoneally. Mice were placed on a dissecting platform, and the thoracic cavity was dissected to expose the heart. After cutting the right atrium using scissors, 15 to 20 ml of phosphate buffered saline (PBS) was slowly injected through the left ventricle. Following PBS perfusion, 15 to 20 ml of 10% buffered formaldehyde saline was slowly injected through the left ventricle. The intact brain, spinal cord, and other tissues were immersed in 10% buffered formalin. The tissues was processed in graded alcohol solutions and embedded in paraffin. These slides were processed for H&E histology staining [59]. Slides that were unstained and used for immunohistochemistry were perfused with 15 to 20 ml of 0.02 M PBS. Following PBS perfusion, 15 to 20 ml of 2% paraformaldehyde was

perfused. This procedure was used for immunohistochemistry in order to retain antigenicity. The spinal cords were isolated and cut transversely through the cervical, thoracic, and lumbar sections. Brains were cut horizontally at the cerebrum, mid-brain, and cerebellum. The tissues were processed in graded alcohol solutions and embedded in paraffin. These slides were then used for immunohistochemical analysis.

Purification of rabbit anti-TMEV antiserum

A solution of 100mg of antigen (GDVII) and .5 M of sodium phosphate ($NaHPO_4$) was prepared. 10mg of antigen per milliliter of sepharose beads was used as recommended by the protocol for a high-capacity column [60,61]. The antigen-bead solution was mixed gently overnight at 4°C on a rocker. The next day the antigen-bead solution was washed gently with 0.5M $NaHPO_4$, 1M sodium chloride (NaCl), and again with 0.05 ethanolamine. The beads were then incubated with 100mM ethanolamine overnight at 4°C on a gentle rocker. The following day the beads were washed with PBS. Anti TMEV antibody was diluted in 10mM of Tris, and then the antibody was passed down the antigen-bead column with a flow rate of approximately 1 ml/hr per each 1ml of column volume. After the antibody was captured on the antigen-bead matrix, the antibodies were washed with 10mM of Tris, 500 mM NaCl, and 10mM if Tris. The antibodies were then eluted by high and low pH washes. The acid pH cycles used 100mM of glycine that contained a pH of 2.5. The solution was then treated with 1M of Tris in order to raise the solution to a basic pH. The elution conditions were kept mild in order to retain the antibody in its native state. Approximately, 0.5ml was collected in separate tubes. The presence of antibody was determined for each tube by

spectroscopy, and tubes with high concentration were combined. The purified antibodies were dialyzed in order to completely remove the elution buffer. Finally, an SDS electrophoresis gel as used in order to confirm the presence of the protein.

Immunohistochemistry

These sections were deparaffinized and 0.02M phosphate-buffered saline containing 0.3% Tween (PBST) used as a rinsing buffer and a dilution buffer. Following incubation with preimmune normal goat serum, the tissues were incubated with rabbit anti-TMEV polyclonal antiserum overnight. The next day the sections were incubated for 45 minutes with the secondary antibody, Goat anti Rabbit IgG (H+L)-biotin followed by 30 min incubation with FITC-streptavidin conjugate. Sections were then washed 3 times for 3 minutes each with PBST. The sections were incubated with prolong gold antifade that contained DAPI. DAPI is a blue fluorochrome that labels nuclei. The sections were then allowed to dry overnight and viewed for immunofluorescence labeling using a fluorescence microscope. The NIF group was incubated with the same protocol as the IF group. The isotype control used was a non-specific rabbit anti IgG antibody. The IF sections were incubated with the secondary antibody only and no primary antibody.

REFERENCES

[1] Vajda FJE. Neuroprotection and neurodegenerative disease. J of Clinical Neuroscience 2002; 9(1): 4-8.

[2] Gilden DH. Infectious causes of multiple sclerosis. Lancet Neurol 2005; 4: 195-202.

[3] Welsh CJR, Blakemore WF, Tonks P, Borrow P, Nash AA. Theiler's murine encephalomyelitis virus infection in mice: a persistent viral infection of the central nervous system which induces demyelination. In: Dimmock NJ, Minor PD, ed. Immune Responses, Virus Infections and Disease. Oxford: Oxford University Press, 1989: 125-147.

[4] Theiler M. Spontaneous encephalomyelitis of mice – A new virus. Science 1934; 80: 122-123.

[5] Lipton HL. Theiler's virus infection in mice: an unusual biphasic disease process leading to demyelination. Infect Immun 1975; 11: 1147-1155.

[6] Oleszak EL, Chang R, Friedman H, Katsetos CD, Platsoucas CD. Theiler's virus infection: a model for multiple sclerosis. Clinical Microbiology Reviews 2004; 17 (1): 174-207.

[7] Fields BN, Knipe DM. Fields Virology, 2nd edn. New York: Raven Press, 1990: 507-548.

[8] Lipton HL, Kumar AS, Trottier M. Theiler's virus persitence in the central nervous system of mice is associated with continuous viral replication and a difference in outcome of infection of infiltrating macrophages versus oligodendrocytes. Virus Res 2005; pending.

[9] van Eyll O, Michiels T. Non – AUG – initiated internal translation of the L* protein of Theiler's virus and importance of this proein for viral persistence. J Virol 2002; 76(21): 10665-73.

[10] Martinat C, Jarousse N, Prevost MC, Brahic M. The GDVII strain of Theiler's virus spreads via axonal transport. J of Vir 1999; 73 (7): 6093-6098.

[11] Rustigian R, Pappenheimer AM. Myositis in mice following intramuscular injection of viruses of the mouse encephalomyelitis group and of certain other neurotropic viruses. J Exp Med 1949; 89: 69-92.

[12] Tsunoda I, Kuang L, Libbey JE, Fujinami RS. Axonal injury heralds virus-

induced demyelination. Amer J of Pathology 2003; 162(4): 1259- 1269.

[13] Adami C, Pritchard AE, Knauf T, Luo M, Lipton H. A determinant for central nervous system persistence localized in the capsid of Theiler's murine encephalomyelitis virus by using recombinant viruses. J of Virology 1998; 72(2): 1662-1665.

[14] Jnaoui K, Minet M, Michiels T. Mutations that affect the tropism of DA and GDVII strains of Theiler's virus in vitro influence sialic acid binding pathogenicity. J of Virology 2002; 76 (16): 8138-8147.

[15] Libbey JE, McCright IJ, Tsunoda I, Wada Y, Fujinami RS. Peripheral nerve protein, PO, as a potential receptor for Theiler's murine encephalomyelitis virus. J of NeuroVirology 2001; 7: 97-104.

[16] Melnick JL, Agol VI, Bachrach HL, Brown F, Cooper PD, Freis W, Gard S, Gear JHS, Ghendon Y, Kasza L, La Placa M, Mandel B, Mc Gregor S, Mohanty S, Plummer G, Rueckert RR, Schaffer FL, Tagaya I, Tyrrell DAJ, Voroshilova M, Wenner HA. Picornaviridae. Intervirology 1974; 4:303.

[17] Bodian D, Hortsmann DM. Polioviruses. In Viral and Rickettsial Infections of Man. 4th edn. In: Horsfall FL Jr, & Tamm I, eds. Philadelphia: Lippincott, 1965: 430-431.

[18] Price RW, Plum F. Poliomyelitis In Handbook of Clinical Neurology, vol. 34, Part III. In: Vinken PJ, Bruyn D, eds. NewYork: North-Holland Pub Com, 1978: 93-94.

[19] Hughes JT. Inflammatory diseases, 2nd edn. In Pathology of the Spinal Cord. London: Lloya-Luke, 1978: 103.

[20] Jurler M, Blasberg RG, Fenstermacher JD, Patlak CS, Paulson OB. A spatial analysis of the blood-brain barrier damage in experimental allergic encephalomyelitis. J Cereb Blood Flow Metab 1985; 5: 545-553.

[21] Zurbriggen A, Fujinami R. Theiler's virus infection in nude mice: Viral RNA in vascular endothelial cells. J Virol 1988; 62: 3589.

[22] Welsh CJR, Sapatino BV, Rosenbaum B, Smith R. Characteristics of cloned cerebrovascular endothelial cells following infection with Theiler's virus in acute infection. J. Neuroimmunology 1995; 62: 119-125.

[23] Freistadt MS, Eberle KE. Hematopoietic cells from CD155-transgenic mice

express CD155 and support poliovirus replication ex vivo. Microb Pathog 2000; 4: 203-212.

[24] Ohka S, Yang W, Terada E, Iwasaki K, Nomoto A. Retrograde transport of intact poliovirus through the axon via the fast transport system. Virology 1998; 250: 67-75.

[25] Wada Y, Fujinami RS. Viral infection and dissemination through the olfactory pathway and the limbic system by Theiler's virus. Amer J of Path 1993; 143 (1): 221-229

[26] Ha-Lee YM, Dillon K, Kosaras B, Sidman R, Revell P, Fujinami R, Chow M. Mode of spread to and within the central nervous system after oral infection of neonatal mice with the DA strain of Theiler's murine encephalomyelitis virus. J of Virology 1995; 69 (11): 7354-7361.

[27] Howe HA, Bosian, D. Poliomyelitis in the chimpanzee: a clinical-pathological study. Bull. Johns Hopkins Hosp 1941; 69:149.

[28] Thompson CB. Apoptosis. In: Paul WE, ed. Fundamental Immunology, 4th ed, Philadelphia: Lippincott- Raven, 1999: 813-29.

[29] Basset C, Holton J, O'Mahony R, Roitt I. Innate immunity and pathogen-host interaction. Vaccine 21 2003; S2/12-S2/23.

[30] Rosenberg HG, Gallin JI. Inflammation. In: Paul WE, ed. Fundamental Immunology, 4th ed, Philadelphia: Lippincott- Raven, 1999: 1051-66.

[31] Gordon S. Macrophages and the Immune Response. In: Paul WE, ed. Fundamental Immunology, 4th edn, Philadelphia: Lippincott- Raven, 1999: 1051-66.

[32] Pachter, J S, De Vires, H E, Fabry, Z: The blood brain barrier and its role in immune privilege in the central nervous system, J of Neuropath and Exp Neur 2003; 62(6): 593-604.

[33] Weller, RO, Engelhardt, B, Phillips, MJ: Lymphocyte targeting of the central nervous system: a review of afferent and efferent CNS-immune pathways. Brain Pathology 1976; 6: 275-288.

[34] Mueller S, Cao X, Welker R, Wimmer E. Interaction of the poliovirus receptor CD155 with the dynein light chain Tctex-1 and its implication for poliovirus pathogenesis. J Biol Chem 2002; 277: 7897-7904.

[35] Ohka S, Matsuda N, Tohyama K, Toshiyuki O, Morikawa M, Kuge S, Nomoto A. receptor (CD155)-dependent endocytosis of poliovirus and retrograde axonal transport of the endosome. J Vir 2004; 78 (13): 7186.

[36] Pfister KK. Cytoplasmic dynein and microtubule transport in the axon: the action connection. Mol Neurobiol 1999; 20(2-3): 81-91.

[37] Kelly RM, Strick PL. Rabies as a transneuronal tracer of circuits in the central nervous system. J of Neuroscience Methods 2000; 103: 63-71.

[38] Marone G, Stephen J, Kitamura G, Kitamura Y. Probing the roles of mast cells and basophils in natural and acquired immunity, physiology and disease. Trends in Immunology 2002; 23 (9): 425-427.

[39] Malaviya R, Georges A. Regulation of mast cell-mediated innate immunity during early response to bacterial infection. Clin ev Allergy Immnol 2002; 22(2): 189-204.

[40] Cheng Qi J, Stevens RL, Wadley R, Collins A, Cooley M, Naif HM, Nasr N, Cunningham A, Katsoulotos G, Wanigasek Y, Roufogalis B, Krilis SA. IL-16 regulation of human mast cells/basophils and their susceptibility to HIV-1. The J of Immunology 2002; 168: 4127-4134.

[41] Rumsaeng V, Cruikshank WW, Foster B, Prussin C, Kirshenbaum AS, Davis TA, Kornfeld H, Center DM, Metcalfe DD. Human mast cells produce the CD4+ T lymphocyte chemoattractant factor, IL-16. J Immunol 1997; 159(6): 2904-10.

[42] Tsunoda I, Kurtz CIB, Fujinami RS. Apoptosis in acute and chronic central nervous system disease induced by Theiler's murine encephalomyelitis virus. Virology 1997; 228: 388-393.

[43] Jelachich ML, Lipton HL. Theiler's murine encephalomyelitis virus kills restrictive but not permissive cells by apoptosis. J Virol 1996; 70(10): 6856-61.

[44] Anderson R, Harting E, Frey MS, Leibowitz JL, Miranda RC. Theiler's murine encephalomyelitis virus induces rapid necrosis and delayed apoptosis in myelinated mouse cerebellar explant cultures. Brain Res 2000; 868(2): 259-67.

[45] Schlitt BP, Felrice M, Jelachich ML, Lipton HL. Apoptotic cells, including macrophages, are prominent in Theiler's murine encephalomyelitis virus-induced inflammatory, demyelinating lesions. J Virol. 2003; 77(7): 4383-8.

[46] Travers JB, Rinaman L. Identification of lingual motor control using two strains of psuedorabies virus. Neuroscience 2002; 4(115): 1139-1151.

[47] Sahara Y, Hashimoto N, Nakamura Y. Hypoglossal premotor neurons in the rostral medullary parvocellular reticular formation participate in cortically-induced rhythmical tongue movements. Neuroscience research 1990; 26: 119-131.

[48] Saper CB. Brain Stem, Reflexive Behavior, and the Cranial Nerves. In: Kandel ER, Schwartz JH, Jessell TM, eds. Principles of Neural Science. New York: McGraw Hill, 2000: 873-88.

[49] Goldberg ME. The Control of gaze. In: Kandel ER, Schwartz JH, Jessell TM, eds. Principles of Neural Science. New York: McGraw Hill, 2000: 789 – 92.

[50] Ugolini G, Kuypers HGJM, Simmons A. Retrograde transneuronal transfer of Herpes simplex virus type 1 (HSV1) from motor neurons. Brain Research 1987; 422: 242-252.

[51] Marson L, Platt KB, McKenna KE. Central nervous system innervation of the penis as revealed by the transneuronal transport of pseudorabies virus. Neuroscience 55 1993; 1: 263-80.

[52] Keane, R.W., Hickey J, ed. Immunology of the Nervous System. New York : Oxford University Press, 1997.

[53] Streilein J W. Ocular immune privilege: therapeutic opportunities from an experiment of nature, Reviews. 2003; 74:179-185.

[54] Streilein J W. Ocular immune privilege: the eye takes a dim but practical view of immunity and inflammation. J of Leukocyte Biology 2003; 74:179-185.

[55] Welsh CJR, Tonks P, Nash AA, Blakemore WF. The effect of L3T4 T cell depletion on the pathogenesis f Theiler's murine encephalomyelitis virus infection in CBA mice. J. Gen. Virol 1987; 68: 1659-1667.

[56] Bervar M. Video analysis of standing – an alternative footprint analysis to access functional loss following injury to the rat sciatic nerve. J of Neuroscience 2000; 102: 109-116.

[57] Walker JL, Evans JM, Resig P, Guarnieri S, Meade P, Sisken BS. Enhancement of functional recovery following a crush lesion to the rat sciatic nerve by exposure to pulsed electromagnetic fields. Experimental Neurology 1994; 125: 302-305.

[58] Walker JL, Evans JM, Meade P, Resig P, Sisken BS. Gait-stance duration as a measure of injury and recovery in the rat sciatic nerve model. J of Neuroscience

Methods 1994; 54: 47-52.

[59] Campbell T, Meagher MW, Sieve A, Scott B, Storts R, Welsh TH, Welsh CJR. The effects of restraint stress on the neuropathogenesis of Theiler's virus infection: I. Acute disease. Brain, Behavior, and Immunity 2001; 15: 235-254.

[60] Harlow E, Lane D. Using Antibodies. Immunoaffinity Purification. New York Cold Spring Harbor Laboratory Press, 1998: 313 – 43.

[61] Harlow E, Lane D. Using Antibodies. Handling Antibodies. New York Cold Spring Harbor Laboratory Press, 1998: 65 - 95.

VITA

Name:	Dorissa Villarreal
Address:	PO Box 665 Brownsville, TX 78520
Email Address:	zeusdv@yahoo.com
Education:	B.S., Biomedical Science, Texas A&M University, 2002